PAF are mediated through a specific G-protein-coupled receptor, PAFR (Honda et al., 1991; Nakamura et al., 1991). A single amino acid substitution (A224D) in the third cytoplasmic loop of human PAFR that modifies its function has been reported, with the variant being relatively common in Japanese, with 13.8% heterozygous and 0.9% homozygous (Fukunaga et al., 2001). Fukunaga et al. also found that Chinese hamster ovary cells expressing A224D mutant PAFR displayed a partial but significant reduction of PAF-induced intracellular signaling, and that the variant exhibited impaired coupling to G-proteins.

The present study aimed to elucidate the effect of the PAFR polymorphism on the development of MS in Japanese; thus, we investigated the PAFR gene polymorphism (A224D) in MS patients, and correlated the findings with clinical parameters.

2. Patients and methods

2.1. Patients

A total of 162 patients (59 men and 103 women) with MS, according to the recommended diagnostic criteria (McDonald et al., 2001), were recruited from the Department of Neurology, Kyushu University Hospital, the Department of Neurology, Hokkaido University Hospital, and the Hokuyukai Neurological Hospital. Hematological and biochemical studies and serologic tests for syphilis were performed in all patients and the results were not contributory. None of the patients was seropositive for human T-cell leukemia virus type 1. Age at examination was 38.2±11.3 years (mean±S.D.) and at disease onset 27.1± 9.9 years (mean±S.D.). Subjects were "conventional" MS patients as described previously (Fukazawa et al., 1992) (i.e., clinical features were similar to those of MS patients in Western countries). Patients with opticospinal MS (OS-MS) whose lesions were clinically confined to the optic nerve and spinal cord were excluded from this study because this group of patients seems to constitute a distinct subgroup (Kira et al., 1996; Yamasaki et al., 1999; Kira, 2003). After at least a 1-year observation period, 120 were diagnosed as relapsing–remitting type MS and 42 as secondary progressive type MS, in which the onset of progressive disease was defined as continual worsening of symptoms and signs for a period at least 6 months, with or without superimposed relapses (Lublin and Reingold, 1996; Confavreux et al., 2000). Primary progressive MS was not included in the present study. MS severity was evaluated by Kurtzke's Expanded Disability Status Scale (EDSS) scores (Kurtzke, 1983) and progression index (PI) (Miyagishi et al., 2003). PI was calculated as a measure of accumulated disability over time (PI=EDSS/disease duration in years). EDSS score was 3.3±2.6 (mean±S.D.) and PI was 0.40±0.42 (mean±S.D.) at the time of examination. The control group was composed of 107 unrelated healthy men and 138 unrelated healthy women (mean age±S.D.= 34.0±10.1 years). Subjects' informed consent was obtained in accord with the declaration of Helsinki, and the ethical committees of the institutions in which the work was performed gave their approval.

2.2. Genotyping of PAFR

Total blood genomic DNA was extracted from leukocytes with a QIAamp DNA Blood Midi Kit (QIAGEN, Tokyo, Japan) following the manufacturer's instructions. The genotype of human PAFR was determined by polymerase chain reaction restriction fragment length polymorphism (PCR-RFLP) according to the method of Fukunaga et al. (2001) without knowledge of the samples' clinical diagnosis. The sense primer used was (5′-CCACAGCGCCC-GGCGCTTGACTGCA-3′) and the antisense primer was (5′-ATCGTGTTCAGCTTCTTCCTGGTCT-3′). Reactions were performed in a total volume of 50 μl containing 0.5 ig of genomic DNA, 20 pmol of each primer, 0.4 mmol/l each of dATP, dGTP, dCTP, and dTTP, 1 U Taq DNA polymerase (Takara, Otsu, Japan), 100 pmol/l KCl , and 20 nmol/l Tris hydrochloride (pH 8.0). The thermocycling procedure consisted of an initial denaturation at 94 °C for 10 min, 30 cycles of 94 °C for 1 min, 58 °C for 1 min, and 72 °C for 1 min. PCR-amplified DNA was digested with *Pst*I (Fukunaga et al., 2001) at 37 °C overnight. PCR products were analyzed by agarose gel (0.7% agarose+2.5% NuSieve) electrophoresis and visualized by ethidium bromide staining. This genetic variant results in the loss of a *Pst*I restriction site; thus, the wild-type allele yielded 105-bp and 24-bp fragments, while the mutant allele remained undigested (129-bp).

2.3. Statistical analysis

Allele and genotype frequencies of the PAFR were compared between MS patients and controls, using chi-square and Fisher's exact tests. Statistical analysis between the genotype PAFR polymorphism (AA vs. AD/DD) and clinical parameters were tested in MS patients, using Mann–Whitney *U* and chi-square tests. Values of $p<0.05$ were considered statistically significant. Statistical analyses were performed with StatView/Mac software.

3. Results

3.1. PAFR genotype and allele frequencies in MS

The proportions of PAFR genotypes (AA, AD, and DD) and alleles (A allele, D allele) in MS patients and healthy controls are shown in Table 1. The frequency of the AD/DD genotypes was significantly higher in MS patients (21.0%) than in healthy controls (13.5%) ($p=0.045$; odds ratio (OR), 1.71; 95% confidence interval (CI), 1.01–2.89). In control

Table 1
Genotype and allele frequency of the PAFR polymorphism in patients with MS and healthy controls

	MS (n=162)	Healthy controls (n=245)
Genotype frequencies		
AA	128 (79.0)[a]	212 (86.5)[a]
AD	30 (18.5)	32 (13.1)
DD	4 (2.5)	1 (0.4)
AD/DD	34 (21.0)[a]	33 (13.5)[a]
Allele frequencies		
A allele	286 (88.3)[b]	456 (93.1)[b]
D allele	38 (11.7)[b]	34 (6.9)[b]

MS=multiple sclerosis. Percentages are in parentheses.
[a] p=0.045; OR, 1.71; 95% CI, 1.01–2.89.
[b] p=0.019; OR, 1.78; 95% CI, 1.10–2.89.

subjects, the genotype frequencies are similar to those found in other Japanese studies (Fukunaga et al., 2001). Moreover, the frequency of D allele in MS patients (11.7%) was also significantly higher than those in healthy controls (6.9%) (p=0.019; OR, 1.78; 95% CI, 1.10–2.89).

3.2. The relation between PAFR polymorphism and clinical parameters

There was no association between the PAFR polymorphism and clinical parameters such as age at onset, sex, clinical phenotype, EDSS, and PI (data not shown).

4. Discussion

In the present study, we disclosed a significant association between susceptibility for MS and the PAFR polymorphism that has a partial but significant reduction of PAF-induced intracellular signaling.

PAF is a proinflammatory mediator produced early in response to several immunological stimuli, including immune complexes and proinflammatory cytokines (Camussi et al., 1981; Valone and Epstein, 1988). Moreover, PAF itself mediates some of the biological effects exerted by cytokines, such as tumor necrosis factor-alpha (TNF-α), interleukin (IL)-1, and IL-8 (Dubois et al., 1989; Poubelle et al., 1991; Denault et al., 1997). Considering the proinflammatory nature of PAF, it is rather unexpected that a missense mutation partially disrupting PAFR signaling is a susceptibility factor for MS. There are two possible explanations for this. First, not all the biological effects of PAF are proinflammatory. It has been shown that PAF is involved in the inhibition of proinflammatory cytokine production during macrophage phagocytosis of apoptotic cells, possibly through the synthesis of transforming growth factor-beta (TGF-β) (Fadok et al., 1998). PAF also suppresses the induction of delayed-type hypersensitivity (DTH) and enhances the transcription of COX-2 and IL-10—two important mediators of systemic immune suppression (Walterscheid et al., 2002). Thus, the missense mutation of PAFR may downmodulate immunosuppressive actions, which then enhance susceptibility for MS in some patients.

Second, PAF preferentially enhances Th2-mediated immune responses (Harada et al., 1996; Kusuhara et al., 2000). Huang et al. (1996) reported that PAF activates Th2 cells to produce IL-4, which is completely inhibited by PAF receptor antagonist. Since activation of Th2 cells inhibit Th1-related cellular immunity, the missense mutation of PAFR may enhance susceptibility for MS, in which Th1 cells are supposed to play a major role, through down-regulation of Th2 cells.

In summary, we analyzed the PAFR polymorphism in Japanese patients, and found that the PAFR AD/DD genotype seems to confer a risk for the development of MS. Further studies on PAF/PAFR signal transduction in MS patients will be necessary to determine whether the PAFR polymorphism is involved in the pathogenesis of MS.

Acknowledgements

We thank Ms. N. Kinukawa (Department of Medical Information Science, Kyushu University Hospital) for help with statistical analyses. This work was supported, in part, by grants from the Ministry of Education, Science, Sports, and Culture of Japan, the Neuroimmunological Disease Research Committee, and the Ministry of Health and Welfare of Japan for Research on Brain Science.

References

Callea, L., Arese, M., Orlandini, A., Bargnani, C., Priori, A., Bussolino, F., 1999. Platelet activating factor is elevated in cerebral spinal fluid and plasma of patients with relapsing–remitting multiple sclerosis. J. Neuroimmunol. 94, 212–221.

Camussi, G., Aglietta, M., Coda, R., Bussolino, F., Piacibello, W., Tetta, C., 1981. Release of platelet-activating factor (PAF) and histamine. II. The cellular origin of human PAF: monocytes, polymorphonuclear neutrophils and basophils. Immunology 42, 191–199.

Chihara, J., Maruyama, I., Yasuba, H., Yasukawa, A., Yamamoto, T., Kurachi, D., Mouri, T., Seguchi, M., Nakajima, S., 1992. Possible induction of intracellular adhesion molecule-1 (ICAM-1) expression on endothelial cells by platelet-activating factor (PAF). J. Lipid Mediat. 5, 159–162.

Confavreux, C., Vukusic, S., Moreau, T., Adeleine, P., 2000. Relapses and progression of disability in multiple sclerosis. N. Engl. J. Med. 343, 1430–1438.

Denault, S., April, M.J., Stankova, J., 1997. Transcriptional activation of the interleukin-8 gene by platelet-activating factor in human peripheral blood monocytes. Immunology 91, 297–302.

Dubois, C., Bissonnette, E., Rola-Pleszczynski, M., 1989. Platelet-activating factor (PAF) enhances tumor necrosis factor production by alveolar macrophages. Prevention by PAF receptor antagonists and lipoxygenase inhibitors. J. Immunol. 143, 964–970.

Fadok, V.A., Bratton, D.L., Konowal, A., Freed, P.W., Westcott, J.Y., Henson, P.M., 1998. Macrophages that have ingested apoptotic cells in vitro inhibit proinflammatory cytokine production through autocrine/

paracrine mechanisms involving TGF-β, PGE2, and PAF. J. Clin. Invest. 101, 890–898.
Fukazawa, T., Miyasaka, K., Tashiro, K., Hamada, T., Moriwaka, F., Yanagihara, T., Hamada, K., 1992. MRI findings of multiple sclerosis with acute transverse myelopathy. J. Neurol. Sci. 110, 27–31.
Fukunaga, K., Ishii, S., Asano, K., Yokomizo, T., Shiomi, T., Shimizu, T., Yamaguchi, K., 2001. Single nucleotide polymorphism of human platelet-activating factor receptor impairs G-protein activation. J. Biol. Chem. 276, 43025–43030.
Harada, M., Sumichika, H., Hamano, S., Ito, O., Tamada, K., Takenoyama, M., Kimura, G., Nomoto, K., 1996. IL-3 derived from $CD4^+$ T cells is essential for the in vitro expansion of mast cells from the normal adult mouse spleen. Clin. Exp. Immunol. 106, 149–155.
Honda, Z., Nakamura, M., Miki, I., Minami, M., Watanabe, T., Seyama, Y., Okado, H., Toh, H., Ito, K., Miyamoto, T., Shimizu, T., 1991. Cloning by functional expression of platelet-activating factor receptor from guinea-pig lung. Nature 349, 342–346.
Huang, Y.H., Schäfer-Flinder, L., Owman, H., Lorentzen, J.C., Rönnelid, J., Frostegard, J., 1996. Induction of IL-4 by platelet-activating factor. Clin. Exp. Immunol. 106, 143–148.
Kira, J., 2003. Multiple sclerosis in the Japanese population. Lancet Neurol. 2, 117–127.
Kira, J., Kanai, T., Nishimura, Y., Yamasaki, K., Matsushita, S., Kawano, Y., Hasuo, K., Tobimatsu, S., Kobayashi, T., 1996. Western versus Asian types of multiple sclerosis: immunogenetically and clinically distinct disorders. Ann. Neurol. 40, 569–574.
Kurtzke, J.F., 1983. Rating neurologic impairment in multiple sclerosis: an Expanded Disability Status Scale (EDSS). Neurology 33, 1444–1452.
Kusuhara, H., Yamaguchi, S., Matsuyuki, H., Sugahara, K., Komatsu, H., Terasawa, M., 2000. Y-24180, an antagonist of platelet-activating factor, suppresses interleukin 5 production in cultured murine Th2 cells and human peripheral blood mononuclear cells. Cytokine 12, 1120–1123.
Lock, C., Hermans, G., Pedotti, R., Brendolan, A., Schadt, E., Garren, H., Langer-Gould, A., Strober, S., Cannella, B., Allard, J., Klonowski, P., Austin, A., Lad, N., Kaminski, N., Galli, S.J., Oksenberg, J.R., Raine, C.S., Heller, R., Steinman, L., 2002. Gene-microarray analysis of multiple sclerosis lesions yields new targets validated in autoimmune encephalomyelitis. Nat. Med. 8, 500–508.
Lublin, F.D., Reingold, S.C., 1996. Defining the clinical course of multiple sclerosis: results of an international survey. Neurology 46, 907–911.
Martin-Mondière, C., Charron, D., Spinnewyn, B., Braquet, P., 1987. MHC in central nervous system: modulation of expression by PAF-acether. Prostaglandins 34, 163.
McDonald, W.I., Compston, A., Edan, G., Goodkin, D., Hartung, H.-P., Lublin, F.D., McFarland, H.F., Paty, D.W., Polman, C.H., Reingold, S.C., Sandberg-Wollheim, M., Sibley, W., Thompson, A., van den Noort, S., Weinshenker, B.Y., Wolinsky, J.S., 2001. Recommended diagnostic criteria for multiple sclerosis: guidelines from the International Panel on the Diagnosis of Multiple Sclerosis. Ann. Neurol. 50, 121–127.
Miyagishi, R., Niino, M., Fukazawa, T., Yabe, I., Kikuchi, S., Tashiro, K., 2003. C–C chemokine receptor 2 gene polymorphism in Japanese patients with multiple sclerosis. J. Neuroimmunol. 145, 135–138.
Nakamura, M., Honda, Z., Izumi, T., Sakanaka, C., Mutoh, H., Minami, M., Bito, H., Seyama, Y., Matsumoto, T., Noma, M., Shimizu, T., 1991. Molecular cloning and expression of platelet-activating factor receptor from human leukocytes. J. Biol. Chem. 266, 20400–20405.
O'Flaherty, J.T., Wykle, R.L., Miller, C.H., Lewis, J.C., Waite, M., Bass, D.A., McCall, C.E., DeChatelet, L.R., 1981. 1-*O*-alkyl-*sn*-glyceryl-3-phosphorylcholines. A novel class of neutrophil stimulants. Am. J. Pathol. 103, 70–79.
Pedotti, R., DeVoss, J.J., Youssef, S., Mitchell, D., Wedemeyer, J., Madanat, R., Garren, H., Fontoura, P., Tsai, M., Galli, S.J., Sobel, R.A., Steinman, L., 2003. Multiple elements of the allergic arm of the immune response modulate autoimmune demyelination. Proc. Natl. Acad. Sci. U. S. A. 100, 1867–1872.
Poubelle, P.E., Gingras, D., Demers, C., Dubois, C., Harbour, D., Grassi, J., Rola-Pleszczynski, M., 1991. Platelet-activating factor (PAF-acether) enhances the concomitant production of tumour necrosis factor-alpha and interleukin-1 by subsets of human monocytes. Immunology 72, 181–187.
Valone, F.H., Epstein, L.B., 1988. Biphasic platelet-activating factor synthesis by human monocytes stimulated with IL-1β, tumor necrosis factor, or IFN-γ. J. Immunol. 141, 3945–3950.
Walterscheid, J.P., Ullrich, S.E., Nghiem, D.X., 2002. Platelet-activating factor, a molecular sensor for cellular damage, activates systemic immune suppression. J. Exp. Med. 195, 171–179.
Wardlaw, A.J., Moqbel, R., Cromwell, O., Kay, A.B., 1986. Platelet-activating factor. A potent chemotactic and chemokinetic factor for human eosinophils. J. Clin. Invest. 78, 1701–1706.
Yamasaki, K., Horiuchi, I., Minohara, M., Kawano, Y., Ohyagi, Y., Yamada, T., Mihara, F., Ito, H., Nishimura, Y., Kira, J., 1999. HLA-DPB1*0501-associated opticospinal multiple sclerosis. Clinical, neuroimaging and immunogenetic studies. Brain 122, 1689–1696.

ELSEVIER

Journal of Neuroimmunology 167 (2005) 170 – 174

Journal of Neuroimmunology

www.elsevier.com/locate/jneuroim

TNF-related apoptosis inducing ligand (TRAIL) gene polymorphism in Japanese patients with multiple sclerosis

Seiji Kikuchi [a], Ryuji Miyagishi [b,*], Toshiyuki Fukazawa [b], Ichiro Yabe [a], Yusei Miyazaki [a], Hidenao Sasaki [a]

[a] *Department of Neurology, Hokkaido University Graduate School of Medicine, Kita-15 Nishi-7, Kita-ku, Sapporo 060-8638, Japan*
[b] *Nishimaruyama Hospital, 7-25, Maruyama Nishimachi 4cho-me, Chuo-ku, Sapporo 064-8557, Japan*

Received 18 January 2005; accepted 24 June 2005

Abstract

TNF-related apoptosis inducing ligand (TRAIL) has been reported to induce apoptosis of autoreactive T cells and other inflammatory cells, and thus, it is a strong candidate gene for involvement in the development of autoimmune diseases. We investigated single nucleotide polymorphisms (SNPs) in the coding region of the gene at position 1595 in exon 5 in 128 Japanese patients with conventional/classical multiple sclerosis (MS) and 158 healthy controls. Patients with optico-spinal MS (OSMS) or atypical clinical attacks were excluded from the study. The frequency of CC genotype at position 1595 was significantly different between patients and controls ($p=0.0027$), and the C allele was more prevalent in the patients than in the controls ($p=0.0138$, OR=1.546, 95% CI=1.092–2.188). Logistic analysis, adjusted for HLA-DRB1*1501-positivity, revealed the independent association of the CC genotype with susceptibility to MS ($p=0.0006$, OR=2.393, 95% CI=1.453–3.943). There were no significant associations between +1595 polymorphism and the clinical features of MS. The results indicate that the presence of the CC genotype at position 1595 in exon 5 represents a higher risk of MS.

Keywords: TRAIL; Multiple sclerosis; Polymorphism; Susceptibility gene; Japanese

1. Introduction

Multiple sclerosis (MS) is an autoimmune disease mediated by T-lymphocytes secreting proinflammatory T helper type 1 (Th1) cytokines, and it is controlled by multiple genes and environmental factors (Vyse and Todd, 1996; Compston and Coles, 2002). Recent genome wide linkage studies demonstrated that MS follows a polygenetic trait with multiple loci being relevant (Ebers et al., 1996; Dumat et al., 2004). The genes involved in polygenic diseases such as MS are not easily identified because clinical manifestation requires several disease-associated alleles of several genes rather than one specific mutation. The analysis of multifactorial diseases such as MS is further complicated by the fact that functional differences of known polymorphisms have not yet been identified.

Apoptosis signaling-related genes are strong candidate genes for involvement in MS because apoptosis is a common regulatory mechanism for normal development and homeostasis of the immune system, and the elimination of autoreactive T cells via apoptosis appears to be impaired in MS (Zipp et al., 1999). Tumor necrosis factor (TNF)-related apoptosis-inducing factor (TRAIL) is a newly identified member of the TNF/nerve growth factor superfamily (Wiley et al., 1995), and preferentially induces apoptosis of various normal cells, such as hepatocytes (Jo et al., 2000), thymocytes (Lamhamedi-Cherradi et al., 2003), neural cells (Nitsch et al., 2000) and oligodendrocytes (Matysiak et al., 2002) as well as tumor cells. TRAIL and its receptors are constitutively expressed in lymphocytes. TRAIL expression in lymphocytes can markedly increase after cell activation (Jeremias et al., 1998; Mariani and

* Corresponding author. Tel.: +81 11 642 4121; fax: +81 11 642 4291.
E-mail address: miyagisi@med.hokudai.ac.jp (R. Miyagishi).

0165-5728/$ - see front matter © 2005 Elsevier B.V. All rights reserved.
doi:10.1016/j.jneuroim.2005.06.021

Krammer, 1998), and the mRNA levels of Fas, Fas ligand and TRAIL are elevated in the peripheral blood mononuclear cells (PBMC) of relapsing-remitting MS patients, while T cell lines established from these patients show a functional defect in the Fas signaling pathway (Comi et al., 2000; Huang et al., 2000; Gomes et al., 2003). Recently, microarray analysis identified a downregulation of TRAIL in MS in Japanese patients (Satoh et al., 2004). Furthermore, TRAIL expression was reported to be a candidate for pretreatment assessment and might be used as a prognostic marker of treatment response to interferon-beta (IFN-b) in MS (Wandinger et al., 2003). IFN-b responders could be distinguished from non-responders by early and sustained induction of TRAIL mRNA, and high concentrations of soluble TRAIL in the sera before treatment may allow the prediction of treatment response.

TRAIL is mapped to the long arm of chromosome 3q26 in humans (Wiley et al., 1995) and is composed of five exons. It encodes approximately 1.77 kb mRNA. Four single nucleotide polymorphisms (SNPs) in the 5′-regulatory region (Wang et al., 2000) as well as four SNPs in the 3′-untranslated region (Unoki et al., 2000; Gray et al., 2001) have been published so far. However, the potential role of the SNPs of the TRAIL gene in susceptibility to MS is not well defined.

The aim of the present study was to analyze the relationships between TRAIL gene polymorphism in the 3′-untranslated region of exon 5 at position 1595 on the mRNA and disease onset, age at disease onset and prognosis in 128 Japanese patients with MS. We chose this particular polymorphism because we could use *Rsa*I restriction enzyme alone. The study also investigated the role of TRAIL gene polymorphism-HLA-DRB1-1501 interaction in the development of MS. This is the first study to investigate possible relationships between MS and TRAIL gene polymorphisms in Japanese patients. Patients with optico-spinal MS (OSMS) were excluded from the present study. Patients with atypical clinical or paraclinical findings (Fukazawa et al., 2003, 2004) were also excluded, and thus, the clinical features of the selected patients were identical to those in Western countries. All subjects studied were residents of Hokkaido, the northernmost island of Japan.

2. Patients and methods

2.1. Patients and healthy individuals

The subjects of this study were 128 unrelated Japanese patients with conventional/classical MS (CMS) who met the inclusion and exclusion criteria described below, and had been observed for at least one year. All patients had experienced two or more clinical attacks and had objective evidence of multiple lesions with no evidence of other disorders. They also fulfilled the diagnostic criteria for MS (McDonald et al., 2001). All patients showed a relapsing-remitting ($n=92$) or secondary progressive course ($n=36$). Patients with neuromyelitis optica (NMO) or optico-spinal MS (OSMS) were excluded. Patients with clinically or paraclinically atypical attacks were also excluded because they have been reported to be a clinically and immunogenetically distinct subtype among patients with a diagnosis of MS (Fukazawa et al., 2003, 2004). The definitions of OSMS and atypical attacks have been described previously (Yamasaki et al., 1999; Fukazawa et al., 2003, 2004). Therefore, all patients in the present study were classified as having conventional/classical MS with involvement of multiple sites in the central nervous system (CNS), including the cerebrum, cerebellum or brainstem, with clinical features similar to those observed in Western countries (Fukazawa et al., 2003, 2004; Weinshenker, 2003).

The female/male ratio was 2.5 : 1. The mean age at blood sampling was 34.8±10.6 years (±SD, range: 16–58). The mean age at disease onset was 26.4±9.2 years (range: 4–54). Each subject was assessed clinically by the Expanded Disability Status Scale (EDSS) (Kurtzke, 1983) using the latest data available. Among the 128 patients, 33 patients were under the treatment of IFN-b at the evaluation of EDSS, and EDSS was evaluated during remitting or slowly progressive phase. The mean age at evaluation of the EDSS was 38.0±11.4 years (range: 18–68). The mean latency between disease onset and EDSS evaluation was 11.6±9.0 years (range: 1–36). The EDSS/disease duration (years) served as an index of disease progression (PI). The mean EDSS was 3.3±2.8 (range: 0–9.5) and the mean PI was 0.46±0.76 (range: 0–7.0). The control group comprised 53 unrelated healthy men and 105 unrelated healthy women (age: 32.8±9.1 years). Both patients and controls were Japanese and were residents of Hokkaido, the northernmost island of Japan. The differences in the sex ratio and age between the patients and the controls were not significant ($p>0.05$).

2.2. Analysis of TRAIL polymorphism

After obtaining written informed consent from each participant, a blood sample was obtained and high molecular weight DNA was extracted from the peripheral blood cells. We examined SNP in the coding region of the gene, a C to T substitution at position 1595 in exon 5, by polymerase chain reaction (PCR)-RFLP. A primer pair of forward (5′-tgagca ctacagcaaa catga-3′) and reverse (5′-gcaccactaaaagatcgcagt-3′) primers generated a 391-bp fragment. This site was recognized by *Rsa*I restriction enzyme (New England Biolabs, Beverly, MA). PCR was performed in a total volume of 20 μl, containing 50 ng of genomic DNA, 10 pmol of each primer, 250 M dNTP, 10 mM KCl, 20 mM Tris–HCl (pH 8.2), 1.5 mM $MgCl_2$ and 0.15 U Taq polymerase (AmpliTaq DNA polymerase; Applied Biosystems, Foster City, CA). The PCR reaction mixtures were then denatured at 95 °C for 5 min, followed by 30 cycles of

denaturation at 94 °C for 1 min, annealing for 1 min at 56 °C, extension at 72 °C for 1 min and final elongation at 72 °C for 10 min. After digesting the PCR products with *Rsa*I for 1 h at 37 °C, alleles of each polymorphic site were determined by 3% agarose gel electrophoresis. The *Rsa*I restriction enzyme detected a dimorphism with bands at 59 and 332 bp (allele C) or at 59, 146 and 186 bp (allele T). DNA typing of DRB1 and DPB1 alleles was analyzed by a non-isotopic oligo-typing method using reverse dot blot hybridization. When the discrimination was not clear using this method, we also used the standard PCR-specific oligonucleotide probe (PCR-SSOP) method (Fukazawa et al., 2000).

2.3. Statistical analysis

Using univariate analyses, allele frequencies and genotype frequencies of the TRAIL gene were compared between MS patients and the controls, using the chi-square test or Fisher's exact test. Relative risks for MS, estimated as the odds ratios [ORs] and 95% confidence intervals (95% CI), were calculated. Then, if we found that candidate alleles at position 1595 may contribute to the risk of MS, confounding influences were assessed in a multiple logistic model. DRB1*1501 positivity was corrected for in the model since DRB1*1501 is a risk factor for conventional MS in Japanese (Fukazawa et al., 2000). We also analyzed the association between TRAIL-polymorphism and age at onset using ANOVA followed by Fisher's protected least significance difference (PLSD). Differences in PI were analysed by the Kruskal–Wallis test. A P value less than 0.05 denoted the presence of a statistically significant difference.

3. Results

3.1. TRAIL genotype and allele frequencies

We successfully determined the type of TRAIL 1595C/T polymorphism in all patients and the controls. The frequencies of the three 1595C/T genotypes are listed in Table 1. We found that the frequency of the CC homozygote in MS patients (51.6%) was significantly higher than in the control (32.3%, $p=0.0027$). The C allele at position 1595 was excessively represented in MS patients (85.3%) compared with the control (69.4%, $p<0.0001$, ORs=2.57, 95% CI=1.65–4.00). The frequency of the C allele in MS patients (69.1%) was significantly higher than the control (59.2%, $p=0.0138$). In the controls, each genotype frequency of 1595C/T polymorphism conformed to Hardy–Weinberg expectations.

Table 1
Genotype and allele frequencies of 1595C/T polymorphism in MS patients and controls

	Controls	MS patients
	$n=158$ (%)	$n=128$ (%)
Genotype frequency[a]		
CC	51 (32.3%)	66 (51.6%)
CT	85 (53.8%)	45 (35.2%)
TT	22 (13.9%)	17 (13.3%)
Allele frequency[b]		
C	187 (59.2%)	177 (69.1%)
T	129 (40.8%)	79 (30.9%)

[a] $p=0.0027$.
[b] $p=0.0138$. ORs (odds ratio)=1.546, 95% CI (confidence interval)=1.092 to 2.188.

Table 2
Odds ratios and 95% CI from multiple logistic analysis

	P value	OR	95% CI
CC genotype (+ vs. −)	0.0006	2.393	1.453 to 3.943
DRB1*1501 allele (+ vs. −)	0.0025	2.435	1.363 to 4.331

After adjusting for the DRB1*1501 allele, the CC genotype and the DRB1*1501 allele were independent risk factors in the logistic regression model.

3.2. Multiple logistic analysis

CC allele frequencies at position 1595 in exon 5 were considered as possible contributors to the risk for MS, and confounding influences were assessed in a logistic regression model. After adjusting for DRB1*1501 positivity, the CC genotype provided an independent risk factor for conventional MS (Table 2).

3.3. Clinical characteristics according to TRAIL genotype status

Among the 128 MS patients, there was no association between position 1595 polymorphism of the TRAIL gene and clinical course (relapsing-remitting course or secondary progressive course). The ages at onset of patients with CC, CT and TT genotypes were 26.4±9.2, 26.4±9.4 and 28.2±11.4 years, respectively. The PI values of patients with CC, CT and TT genotypes were 0.371±0.392, 0.354±0.412 and 0.414±0.517, respectively. There were no associations between genotypes of these genes and the age at disease onset or the PI.

4. Discussion

The major finding of the present study was that the presence of the CC genotype at position 1595 in exon 5 indicated a higher risk of MS, but it was not associated with the clinical course, age at disease onset or disability index.

A previous study using reverse transcription-PCR (RT-PCR) analysis showed elevated TRAIL mRNA levels in peripheral blood lymphocytes in MS (Huang et al., 2000), while a recent study showed low serum levels of soluble TRAIL in relapsing-remitting MS (Wandinger et al., 2003).

It remains to be determined whether TRAIL expression represents a disease-promoting autoimmune process or merely the effect of a secondary compensatory mechanism that downregulates the inflammatory response. Indeed, blockade of TRAIL expressed in CD4+ myelin-specific T cells reduced caspase-dependent neuronal cell death and markedly ameliorated clinical severity in experimental autoimmune encephalomyelitis (EAE) (Aktas et al., 2001). Adult human oligodendrocytes were reported to have TRAIL receptors and TRAIL-induced oligodendrocyte apoptosis (Matysiak et al., 2002). In contrast, blocking endogenous TRAIL with soluble TRAIL receptor exacerbated EAE (Hilliard et al., 2001). These findings suggest a two-edged role for TRAIL in MS by promoting both destructive and anti-inflammatory properties.

As stated above, our results showed that the presence of the CC genotype at position 1595 in exon 5 indicated a higher risk of MS. However, the mechanism by which TRAIL polymorphism in the 3′ UTR region influences the pathogenesis of MS is not clear at present. Recently, a highly polymorphic region in the TRAIL promoter was demonstrated but it did not influence TRAIL expression, MS susceptibility or the clinical disease pattern (Weber et al., 2004). Investigation into whether and how 3′ UTR polymorphism influences the expression of TRAIL mRNA is desired for assessing the relevance of our results. Furthermore, other SNPs of TRAIL gene rather than SNP at position 1395 should be investigated for possible association with MS.

IFN-b has demonstrated benefits in the treatment of patients with MS. It is reported that TRAIL expression might be used as a prognostic marker of treatment response to IFN-b in MS (Wandinger et al., 2003). Drug-responders could be distinguished from non-responders by early and sustained induction of TRAIL. Among the 128 patients in the current study, 33 patients were under the treatment of IFN-b. Although our sample size was small, no association was detected between +1595 polymorphism and the efficacy of IFN-b (data not shown).

The prevalence rates of MS in Japan and Asian countries are significantly lower than those in European and North American countries. In a series of our recent studies, we reported the association of various gene polymorphisms in Japanese patients with MS (Fukazawa et al., 1999; Niino et al., 2000, 2002, 2003; Kikuchi et al., 2002; Miyagishi et al., 2003). Some of our results were not consistent with those of Western countries, and this inconsistency may be due, in part, to differences in the polymorphisms derived from different ethnic backgrounds. Regarding TRAIL gene polymorphism, the frequency of the C allele at position 1595 was 0.592 in the Japanese population, compared with 0.712 in American Caucasians (Gray et al., 2001). Further analysis in other ethnic populations should provide important insights and clues about the genetic and clinical heterogeneity of MS (Oksenberg et al., 2001).

In summary, the present study shows that polymorphism at position 1595 of the TRAIL gene is associated with MS susceptibility in Japanese patients. Our sample size was relatively small, and thus further studies of a large number of subjects are necessary to determine the role of TRAIL polymorphism in the pathogenesis of MS. Moreover, it is warranted to resolve the mechanism by which TRAIL polymorphism in 3′ UTR region influences MS pathogenesis.

Acknowledgements

This work was supported, in part by a research grant from the Research on Brain Science, from the Ministry of Health, Labor and Welfare of Japan, and by a research grant from the Research Committee on the Neuroimmunological Disorders, from the Ministry of Health, Labor and Welfare of Japan.

References

Aktas, O., Osmanova, V., Beyer, M., Brocke, S., Zipp, F., 2001. Therapeutic modulation of the TRAIL system in autoimmune CNS inflammation. J. Neuroimmunol. 118, 52 (Abstract).

Comi, C., Leone, M., Bonissoni, S., DeFranco, S., Bottarel, F., Mezzatesta, C., Chiocchetti, A., Perla, F., Monaco, F., Dianzani, U., 2000. Defective T cell Fas function in patients with multiple sclerosis. Neurology 55, 921–927.

Compston, A., Coles, A., 2002. Multiple sclerosis. Lancet 359, 1221–1231.

Dumat, D.A., Ebers, G.C., Sadovnick, A.D., 2004. Genetics of multiple sclerosis. Lancet Neurol. 3, 104–110.

Ebers, G.C., Kukay, K., Bulman, D.E., Sadovnick, A.D., Rice, G., Anderson, C., Armstrong, H., Cousin, K., Bell, R.B., Hader, W., Paty, D.W., Hashimoto, S., Oger, J., Duquette, P., Warren, S., Gray, T., O'Connor, P., Nath, A., Auty, A., Metz, L., Francis, G., Paulseth, J.E., Murray, T.J., Pryse-Phillips, W., Risch, N., 1996. A full genome search in multiple sclerosis. Nat. Genet. 13, 472–476.

Fukazawa, T., Yabe, I., Kikuchi, S., Sasaki, H., Hamada, T., Miyasaka, K., Tashiro, K., 1999. Association of vitamin D receptor gene polymorphism with multiple sclerosis in Japanese. J. Neurol. Sci. 166, 47–52.

Fukazawa, T., Yamasaki, K., Ito, H., Kikuchi, S., Minohara, M., Horiuchi, I., Tsukishima, E., Sasaki, H., Hamada, T., Nishimura, Y., Tashiro, K., Kira, J., 2000. Both the HLA-CPB1 and -DRB1 alleles correlate with risk for multiple sclerosis in Japanese: clinical phenotypes and gender as important factors. Tissue Antigens 55, 199–205.

Fukazawa, T., Kikuchi, S., Niino, M., Yabe, I., Hamada, T., Tashiro, K., 2003. Multiphasic demyelinating disorder with acute transverse myelitis in Japanese. J. Neurol. 250, 624–626.

Fukazawa, T., Kikuchi, S., Niino, M., Yabe, I., Miyagishi, R., Fukaura, H., Hamada, T., Tashiro, K., Sasaki, H., 2004. Attack-related severity. A key factor in understanding the spectrum of idiopathic inflammatory demyelinating disorders. J. Neurol. Sci. 225, 71–78.

Gomes, A.C., Jonsson, G., Mjomheim, S., Olsson, T., Hillert, J., Grandien, A., 2003. Upregulation of the apoptosis regulators cFLIP, CD95 and CD95 ligand in peripheral blood mononuclear cells in relapsing-remitting multiple sclerosis. J. Neuroimmunol. 135, 126–134.

Gray, H.L., Sorensen, E.L., Hunt, J.S., Ober, C., 2001. Three polymorphisms in the 3′ UTR of the TRAIL (TNF-related apoptosis-inducing ligand) gene. Genes Immun. 2, 469–470.

Hilliard, B., Wilmen, A., Seidel, C., Liu, T.S., Goke, R., Chen, Y., 2001. Roles of TNF-related apoptosis-inducing ligand in experimental autoimmune encephalomyelitis. J. Immunol. 166, 1314–1319.

Huang, W.X., Huang, M.P., Gomes, M.A., Hillert, J., 2000. Apoptosis mediators fasL and TRAIL are upregulated in peripheral blood mononuclear cells in MS. Neurology 55, 928–934.

Jeremias, I., Herr, I., Boehler, T., Debatin, K.M., 1998. TRAIL/Apo-2-ligand-induced apoptosis in human T cells. Eur. J. Immunol. 28, 143–152.

Jo, M., Kim, T.H., Seol, D.W., Esplen, J.E., Dorko, K., Billiar, T.R., Strom, S.C., 2000. Apoptosis induced in normal human hepatocytes by tumor necrosis factor-related apoptosis-inducing ligand. Nat. Med. 6, 564–567.

Kikuchi, S., Fukazawa, T., Niino, M., Yabe, I., Miyagishi, R., Hamada, T., Tashiro, K., 2002. Estrogen receptor gene polymorphism and multiple sclerosis in Japanese patients: interaction with HLA-DRB1*1501 and disease modulation. J. Neuroimmunol. 128, 77–81.

Kurtzke, J.F., 1983. Rating neurologic impairment in multiple sclerosis: an expanded disability status scale (EDSS). Neurology 33, 1444–1452.

Lamhamedi-Cherradi, S.E., Zheng, S.J., Maguschak, K.A., Peschon, J., Chen, Y.H., 2003. Defective thymocyte apoptosis and accelerated autoimmune diseases in TRAIL−/− mice. Nat. Immunol. 4, 255–260.

Mariani, S.M., Krammer, P.H., 1998. Surface expression of TRAIL/Apo-2 ligand in activated mouse T and B cells. Eur. J. Immunol. 28, 1492–1498.

Matysiak, M., Jurewicz, A., Jaskolski, D., Selmaj, K., 2002. TRAIL induces death of human oligodendrocytes isolated from adult brain. Brain 125, 2469–2480.

McDonald, W.I., Compston, A., Edan, G., Goodkin, D., Hartung, H.P., Lublin, F.D., McFarland, H.F., Paty, D.W., Polman, C.H., Reingold, S.C., Sandberg-Wollheim, M., Sibley, W., Thompson, A., van den Noort, S., Weinshenker, B.Y., Wolinsky, J.S., 2001. Recommended diagnostic criteria for multiple sclerosis: guidelines from the International Panel on the diagnosis of multiple sclerosis. Ann. Neurol. 50, 121–127.

Miyagishi, R., Niino, M., Fukazawa, T., Yabe, I., Kikuchi, S., Tashiro, K., 2003. C-C chemokine receptor 2 gene polymorphism in Japanese patients with multiple sclerosis. J. Neuroimmunol. 145, 135–138.

Niino, M., Fukazawa, T., Yabe, I., Kikuchi, S., Sasaki, H., Tashiro, K., 2000. Vitamin D receptor gene polymorphism in multiple sclerosis and the association with HLA class II alleles. J. Neurol. Sci. 177, 65–71.

Niino, M., Kikuchi, S., Fukazawa, T., Miyagishi, R., Yabe, I., Tashiro, K., 2002. An examination of the Apo-1/Fas promoter Mva I polymorphism in Japanese patients with multiple sclerosis. BMC Neurol. 2, 8.

Niino, M., Kikuchi, S., Fukazawa, T., Yabe, I., Tashiro, K., 2003. Genetic polymorphisms of osteopontin in association with multiple sclerosis in Japanese patients. J. Neuroimmunol. 136, 125–129.

Nitsch, R., Bechmann, I., Deisz, R.A., Haas, D., Lehmann, T.N., Wendling, U., Zipp, F., 2000. Human brain-cell death induced by tumour-necrosis-factor-related apoptosis-inducing ligand (TRAIL). Lancet 356, 827–828.

Oksenberg, J.R., Baranzini, S.E., Barcellos, L.F., Hauser, S.L., 2001. Multiple sclerosis: genomic rewards. J. Neuroimmunol. 113, 171–184.

Satoh, J., Nakanishi, M., Koike, F., Miyake, S., Yamamoto, T., Kawai, M., Kikuchi, S., Nomura, K., Yokoyama, K., Ota, K., Kanda, T., Fukazawa, T., Yamamura, T., 2004. Microarray analysis identifies an aberrant expression of apoptosis and DNA damage-regulatory genes in multiple sclerosis. Neurobiol. Dis. 18, 537–550.

Unoki, M., Furuta, S., Onouchi, Y., Watanabe, O., Doi, S., Fujiwara, H., Miyatake, A., Fujita, K., Tamari, M., Nakamura, Y., 2000. Association studies of 33 single nucleotide polymorphisms (SNPs) in 29 candidate genes for bronchial asthma: positive association a T924C polymorphism in the thromboxane A2 receptor gene. Hum. Genet. 106, 440–446.

Vyse, T.J., Todd, J.A., 1996. Genetic analysis of autoimmune disease. Cell 85, 311–388.

Wandinger, K.P., Lunemann, J.D., Wengert, O., Bellmann-Strobl, J., Aktas, O., Weber, A., Grundstrom, E., Ehrlich, S., Wernecke, K.D., Volk, H.D., Zipp, F., 2003. TNF-related apoptosis inducing ligand (TRAIL) as a potential response marker for interferon-beta treatment in multiple sclerosis. Lancet 361, 2036–2043.

Wang, Q., Ji, Y., Wang, X., Evers, B.M., 2000. Isolation and molecular characterization of the 5′-upstream region of the human TRAIL gene. Biochem. Biophys. Res. Commun. 276, 466–471.

Weber, A., Wandinger, K.P., Mueller, W., Aktas, O., Wengert, O., Grundstrom, E., Ehrlich, S., Windemuth, C., Kuhlmann, T., Wienker, T., Bruck, W., Zipp, F., 2004. Identification and functional characterization of a highly polymorphic region in the human TRAIL promoter in multiple sclerosis. J. Neuroimmunol. 149, 195–201.

Weinshenker, B.G., 2003. Neuromyelitis optica: what it is and what it might be. Lancet 361, 889–890.

Wiley, S.R., Schooley, K., Smolak, P.J., Din, W.S., Huang, C.P., Nicholl, J.K., Sutherland, G.R., Smith, T.D., Rauch, C., Smith, C.A., et al., 1995. Identification and characterization of a new member of the TNF family that induces apoptosis. Immunity 3, 673–682.

Yamasaki, K., Horiuchi, I., Minohara, M., Kawano, Y., Ohyagi, Y., Yamada, T., Mihara, F., Ito, H., Nishimura, Y., Kira, J., 1999. HLA-DPB1*0501 associated optico-spinal multiple sclerosis: clinical, neuroimaging and immunogenetic studies. Brain 122, 1689–1696.

Zipp, F., Krammer, P.H., Weller, M., 1999. Immune (dys)regulation in multiple sclerosis: role of the CD95–CD95 ligand system. Immunol. Today 20, 550–554.

"OSMS is NMO, but not MS": confirmed by NMO-IgG?

The debate continues about whether opticospinal multiple sclerosis (OSMS) is MS or not. Lennon and colleagues[1] recently reported the biomarker for neuromyelitis optica (NMO), NMO-IgG, and concluded that it is specific to NMO. The researchers assert that this is proof that "NMO is not MS", that the antibody can distinguish NMO from MS, and that Asian OSMS seems to be the same as NMO.

Lennon and colleagues[1] tested serum samples of 102 North American patients with NMO or with syndromes that suggest high risk of the disorder and 12 Japanese patients with OSMS. In a recent report by Cree and co-workers,[2] most African and European American patients with OSMS did not meet criteria for NMO and had brain lesions on MRI. The 12 Japanese patients with OSMS in Lennon's study fulfilled the criteria for NMO set by Wingerchuck and colleagues.[3] Therefore, Lennon and colleagues elucidated the existence of NMO in Japan; and it is important of course that the presence of NMO-IgG is viewed with the same importance in both Japan and the USA. The patients said to have Japanese OSMS in Lennon and colleagues' study do not actually have Japanese OSMS.

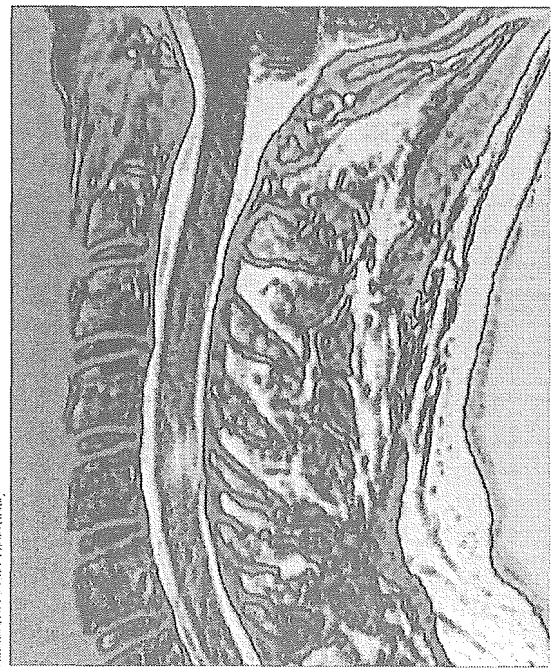

Clinical definitions of OSMS, MS, and NMO complicated by overlap of signs

Lennon and colleagues emphasised that NMO-IgG can definitely discriminate NMO from MS. If so, what is the key feature that produces different results of NMO-IgG positivity? NMO-IgG positivity tends to increase from MS high-risk syndrome to NMO. This continuity suggests that NMO-IgG positivity is part of variation within the MS spectrum and that NMO-IgG-positive patients comprise a unique subgroup of patients with MS. Patients with high-risk syndrome can develop either NMO or MS in the future, and most of them have atypical MS in the Lennon and colleagues classification, because they have extensive spinal-cord lesions or have recurrent optic neuritis. Lennon and colleagues did not mention the clinical features of MS, nor did they mention the presence of extensive spinal-cord lesion on MRI in MS. It will be crucial to check NMO-IgG in typical patients with MS who have extensive spinal-cord lesions. NMO-IgG positivity may be a biological marker indicating the tendency of lesion expansion rather than unique lesion distribution. Furthermore, whether or not recurrent optic neuritis is positive for NMO-IgG is unknown.

The relation between observational characteristics (NMO-IgG in this case) and definition of disorders is determined in a mutually dependent manner. When patients positive for NMO-IgG alone are collected and designated as NMO, both the sensitivity and specificity approach 100% by tautology. After such a procedure, we do not know how to classify NMO-IgG-negative NMO: is this atypical NMO or is this another clinical entity? Actually, Wingerchuk and colleagues[4] made amendments to the NMO criteria at this year's American Academy of Neurology meeting, in which they removed the requirement for no clinical evidence of neurological disease outside the optic nerves and spinal cord from the diagnostic criteria.

There are some other important issues to be resolved in Lennon and colleagues' study. NMO-IgG does not explain the characteristic lesion distribution in NMO, because NMO-IgG reacts in cerebellum and midbrain slices as well as spinal cord. NMO-IgG may be a reflection of the tendancy for European patients with NMO to have high titres autoantibodies. Severe perivascular inflammation in NMO may release aquaporin-4 (which was recently shown to be a possible target antigen of NMO-IgG) from tissues and secondarily induce aquaporin-4 antibody.[5]

Lennon and colleagues[1] insisted that NMO is not MS and that OSMS is identical to NMO, inferring that OSMS is not MS. However, in Japan, OSMS is designated as a variant of MS. The justifications of both opinions are not made a priori. Our position that OSMS is a variant of MS, however, has some advantages in investigation of Asian MS, because in the MS Forum Asia held in Bangkok and Ho Chi Minh 2 years ago, it was confirmed that there are many cases labelled as OSMS in Asia. We believe that the designation of OSMS is useful until we can obtain sufficient data about the epidemiology, natural history, and treatment of this disorder. Recently, Cree and co-workers[6] and Saida and colleagues[7] demonstrated the effectiveness of rituximab for refractory NMO, and interferon beta-1b for OSMS, respectively. At present, it is too early to conclude that interferon beta is ineffective in preventing relapses in NMO or OSMS, and large scale randomised controlled trials are warranted.

Seiji Kikuchi, Toshiyuki Fukazawa
Department of Neurology, Hokkaido University Graduate School of Medicine (SK), and Department of Neurology, Nishimaruyama Hospital (TF) Sapporo, Japan skikuti@med.hokudai.ac.jp

We have no conflicts of interest.

1 Lennon VA, Wingerchuk DM, Kryzer TJ, et al. A serum autoantibody marker of neuromyelitis optica: distinction from multiple sclerosis. *Lancet* 2004; **364:** 2106–12.
2 Cree BAC, Khan O, Bourdette D, et al. Clinical characteristics of African Americans vs Caucasian Americans with multiple sclerosis. *Neurology* 2004; **63:** 2039–45.
3 Wingerchuk DM, Hogancamp WF, O'Brien PC, et al. The clinical course of neuromyelitis optica (Devic's syndrome). *Neurology* 1999; **53:** 1107–14.
4 Wingerchuk DM, Scottsdale AZ, Pittock SJ, et al. Neuromyelitis optica diagnostic criteria revised: validation and incorporation of the NMO-IgG serum autoantibody. *Neurology* 2005; **64** (suppl 1): A38
5 Lennon VA, Kryzer TJ, Pittock SJ, et al. IgG marker of optic-spinal multiple sclerosis binds to the aquaporin-4 waterchannel. *J Exp Med* 2005; **202:** 473–77.
6 Cree BAC, Lamb S, Morgan K, et al. An open label study of the effects of rituximab in neuromyelitis optica. *Neurology* 2005; **64:** 1270–72.
7 Saida T, Tashiro K, Itoyama Y, et al. Interferon beta-1b is effective in Japanese RRMS patients. A randomized, multicenter study. *Neurology* 2005; **64:** 621–30.

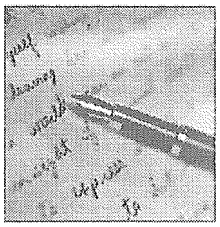

Available online at www.sciencedirect.com
SCIENCE DIRECT
ELSEVIER
Biochemical and Biophysical Research Communications 340 (2006) 263–267
BBRC
www.elsevier.com/locate/ybbrc

In vivo delivery of small interfering RNA targeting brain capillary endothelial cells

Taro Hino [a,1], Takanori Yokota [a,*], Shingo Ito [b], Kazutaka Nishina [a], Young-Sook Kang [b,c], Shinobu Mori [b], Satoko Hori [b], Takashi Kanda [a], Tetsuya Terasaki [b], Hidehiro Mizusawa [a,1]

[a] *Department of Neurology and Neurological Science, Graduate School, Tokyo Medical and Dental University, Tokyo, Japan*
[b] *Department of Molecular Biopharmacy and Genetics, Graduate School of Pharmaceutical Sciences, Tohoku University, Sendai, Japan*
[c] *College of Pharmacy, Sookmyung Women's University, Seoul, Republic of Korea*

Received 24 November 2005
Available online 9 December 2005

Abstract

Brain capillary endothelial cells (BCECs) play an important role in blood–brain barrier (BBB) functions and pathophysiologic mechanisms in brain ischemia and inflammation. We try to suppress gene expression in BCECs by intravenous application of small interfering RNA (siRNA). After injection of large dose siRNA with hydrodynamic technique to mouse, suppression of endogenous protein and the BBB function of BCECs was investigated. The brain-to-blood transport function of organic anion transporter 3 (OAT3) that expressed in BCECs was evaluated by Brain Efflux Index method in mouse. The siRNA could be delivered to BCECs and efficiently inhibited endogenously expressed protein of BCECs. The suppression effect of siRNA to OAT3 is enough to reduce the brain-to-blood transport of OAT3 substrate, benzylpenicillin at BBB. The in vivo siRNA-silencing method with hydrodynamic technique may be useful for the study of BBB function and gene therapy targeting BCECs.

Keywords: Small interfering RNA; Blood–brain barrier; Organic anion transporter 3; Brain ischemia; Brain inflammation; Drug delivery system

In brain ischemia and inflammation, the brain capillary endothelial cells (BCECs) have no longer been regarded as an inert vascular lining that is injured and morphologically changed, but actively play many important roles of these pathophysiologic mechanisms. The inhibition of signaling molecule in BCECs of vascular endothelial growth factor (VEGF)-induced vasogenic edema can reduce an ischemic lesion [1]. The inflammatory cell adhesion molecules expressed in BCECs induced by ischemia, such as intercellular adhesion molecule (ICAM) and E-selectin, can be a target molecule [2,3] for the therapy of these diseases. Because leukocytes activation and adhesion to BCECs are believed to contribute to additional, secondary neuronal injury after reperfusion [4] and initiate immune-mediated encephalopathy such as multiple sclerosis [5]. Endothelial nitric oxide synthases expressed in BCECs are also a possible target molecule. In cerebral ischemia, nitric oxide is increased and works as a prooxidant via peroxynitrite [6]. Therefore, BCECs are an important platform in the cerebral ischemia and inflammation, and express many constitutively or transiently expressed molecules which might be a therapeutic target for these pathologies.

RNA interference is a powerful tool for post-transcriptional gene silencing. Recently, we showed an in vitro model whose function of the transporter protein expressed in BCECs is inhibited by siRNA [7]. Here, we try to introduce siRNA by hydrodynamic, intravenous injection method from mouse tail vein and investigate the siRNA effect on brain-to-blood transport function by inhibiting organic anion transporter 3 (OAT3) with Brain Efflux Index method.

* Corresponding author. Fax: +81 3 5803 0169.
E-mail address: tak-yokota.nuro@tmd.ac.jp (T. Yokota).
[1] 21st century COE Program on Brain Integration and it's Disorders.

0006-291X/$ - see front matter © 2005 Elsevier Inc. All rights reserved.
doi:10.1016/j.bbrc.2005.11.173

Materials and methods

Effect of siRNA on expression of recombinant OAT3 in culture cells. The mOAT3cDNA was subcloned from pGEM-HEN/Roct (OAT3) [8] into the *Renilla* luciferase expression vector, psiCHECK-1 (Promega).

Human embryonic kidney 293 (HEK293) cells were transfected with 80 ng of *Renilla* luciferase-fused OAT3 expression vector, 20 ng of *firefly* luciferase expression vector (pGL3; Promega), and 25 nM siRNA in each well of 24-well plates. *Renilla* luciferase activity was normalized with *firefly* luciferase activity. The luciferase activities were analyzed after 24 h after transfection using the Dual Luciferase System (Promega).

Effect of siRNA on uptake of OAT3 substrate in culture cells. The mOAT3 cDNA was subcloned into the pcDNA3 vector. HEK293 cells in 6-well plates were transfected by 0.5 μg of pcDNA3/OAT3 or vector alone with 100 nM siRNA using the Lipofectamine 2000 (Invitrogen). Twenty-four hours after transfection, the cells were passaged into the 24-well plates, and after another 24 h the cells were washed with phosphate-buffered saline (PBS). The uptake study was initiated at 37 °C by applying 200 μl PBS containing 0.5 μCi [^{3}H]benzylpenicillin to estimate the volume of adherent water. After incubation for 2 min, the radioactivities of ^{3}H in the cells were measured. The uptake of [^{3}H]benzylpenicillin was expressed as the ratio to control siRNA (shuffle sequence).

Animals. Adult male of Institute of Cancer Research (ICR) mice, weighing 35–42 g and age 9–10 weeks, were purchased from Charles River Laboratories. All experiments were approved by the Animal Experiment Committee of Tokyo Medical and Dental University.

In vivo transduction of siRNA with hydrodynamic injection method. Hydrodynamic injection method has been performed according to a previously reported method in mice [9]. The 50 μg siRNA in a volume equivalent to 5–10% of the body weight was rapidly injected in 3–5 s into the mouse tail vein. For comparison, the same amount of siRNA in 0.2 ml PBS was injected slowly in more than 60 s into the mouse tail vein as a regular intravenous injection method.

Brain small vascular fractionation and Western blot analysis. Mice brains were harvested 24 h after application of 50 μg siRNA SOD1 with the hydrodynamic or regular injection method. The total brain homogenate [10] and the brain vascular fraction of small vessels were prepared using a modified method reported previously [11]. Briefly, brains were homogenized in Dulbecco's modified Eagle's medium (DMEM). The homogenates were dissociated further with 0.005% (wt/vol) dispase (grade 1; Roche Diagnostic) at 37 °C for 2 h. After centrifugation (800*g*, 5 min), the pellets were suspended with a dextran solution (M_w 70,000; 15% wt/vol; Sigma) and centrifuged (4 °C, 4500*g* for 10 min). The pellets were resuspended with 0.05 M PBS for 10 min. After centrifugation (800*g*, 5 min), the final pellets of small vessels were resuspended in lysis buffer (20 mM Tris–HCl, 0.1% SDS, and 1% Triton).

Fractionated mouse brain tissues and mouse brain capillary endothelial cell line [12] cells were homogenized in buffer containing 10 mM Tris–HCl (pH 7.4), 1 mM EDTA, 150 mM NaCl, 4% Chaps, 1 mM phenylmethylsulfonyl fluoride (PMSF), and a protease-inhibitor cocktail (Complete-Mini; Roche Diagnostic). The 2.5 μg samples were separated with 7.5% SDS–polyacrylamide mini-gel (Bio-Rad) and transferred to a polyvinylidene difluoride membrane. The membrane was probed with anti-glucose-transporter-1 antibodies (Alpha Diagnostic International) or anti-SOD1 antibodies (Stressgen Biotechnologies) and visualized by using an ECL Western blot system (Amersham–Pharmacia).

Assay for efflux function of OAT3 in vivo. Fifty micrograms of siRNA OAT3 or control siRNA was delivered to brain capillary endothelial cells with hydrodynamic injection via the tail vein. After 36 h, the in vivo brain efflux experiments were carried out using Brain Efflux Index (BEI) method as described previously [13]. Each mouse was anesthetized intramuscularly with a mixture of ketamine (125 mg/kg) and xylazine (1.22 mg/kg), then mounted on a stereotaxic frame (SRS-6; Narishige), to hold the head in position. Using a dental drill, a bore hole was made 3.8 mm lateral to the bregma. Then, extracellular fluid buffer (122 mM NaCl, 25 mM $NaHCO_3$, 3 mM KCl, 1.4 mM $CaCl_2$, 1.2 mM $MgSO_4$, 0.4 mM K_2HPO_4, 10 mM D-glucose, and 10 mM Hepes, pH 7.4) containing 96 nCi [^{3}H]benzylpenicillin and 4.8 nCi [^{14}C]inulin was injected over a period 1 min using a 5.0-μl microsyringe (Hamilton Reno) fitted with a fine needle at a depth of 2.5 mm from the surface of the scalp, i.e., the secondary somatosensory cortex 2 (S2) region. The needle was left in this configuration for an additional 4 min to prevent reflux of the injected solution along the injection track, before being slowly retracted. After 40 min, the whole brain was subsequently removed and the left cerebrum was isolated. After weighing each of these, tissue samples were solubilized in 2 N NaOH at 60 °C for 1 h and then mixed with Hionic-fluor (Packard). The radioactivity in each sample was assayed in a liquid scintillation counter equipped with an appropriate crossover correction for ^{3}H and ^{14}C (LS-6500; Beckman).

The BEI was defined by Eq. (1) and the percentage of substrate remaining in the ipsilateral cerebrum was determined from Eq. (2).

$$\mathrm{BEI}(\%) = \frac{\text{test substrate undergoing efflux at the BBB}}{\text{test substrate injected into the brain}} \times 100 \quad (1)$$

$$\text{100-BEI}(\%) = \frac{(\text{amount of test substrate in the brain}/\text{amount of reference in the brain})}{(\text{concentration of test substrate injected}/\text{concentration of reference injected})} \times 100. \quad (2)$$

The percentage of [^{3}H]benzylpenicillin remaining in the brain is given by (100-BEI).

The data were used when the remaining amount of [^{14}C]inulin in the brain was more than 15% of the injected amount. No significant difference was observed in the remaining percentage of [^{14}C]inulin, which is a non-permeable marker, among all samples (#1, 39.7 ± 3.5%; #2, 27.5 ± 3.4%; #3, 31.4 ± 2.9%; #2 shuffle, 28.9 ± 2.2%) (ANOVA), showing that the hydrodynamic injection of siRNA did not damage the integrity of BBB.

Data analysis. All data represent means ± SEM. An unpaired, two-tailed Student's *t* test was used to determine the significance of differences between two group means. (The difference is certified when $P < 0.05$.)

Results

siRNA directed against the OAT3 and SOD1 genes

Sense sequences of the siRNA designed to OAT3 and SOD1 genes are described as follows. The siRNA of shuffle sequence of siRNA OAT3 #2 and siRNA against unrelated gene, GBV-B virus, were used as negative controls. Uppercase letters at 3′ end indicate deoxyribonucleotides.

siRNA OAT3 #1:	5′-ucuacaacagcaccagagaTT-3′
siRNA OAT3 #2:	5′-ccauuaucuugaauguggaTT-3′
siRNA OAT3 #3:	5′-aaacaaagcaggagccagaTT-3′
siRNA-shuffle sequence:	5′-agugguaaugucuauauccTT-3′
siRNA-unrelated control:	5′-agugguaaugucuauauccTT-3′
siRNA SOD1:	5′-gguggaaaugaagaaaguaTT-3′

Effect of siRNA on expression and function of recombinant OAT3 in culture cells

siRNA OAT3 #2 most effectively reduced the expression of OAT3 in HEK293 cells by 86.2% on luciferase activity compared with control siRNA with shuffle sequence of siRNA OAT3 #2 (Fig. 1). siRNA OAT3 #1 and #3 were moderately effective.

To investigate the inhibition effect of siRNA OAT3 to its efflux function in vitro, we measured uptake of OAT3 substrate, [^{3}H]benzylpenicillin. After expression of OAT3

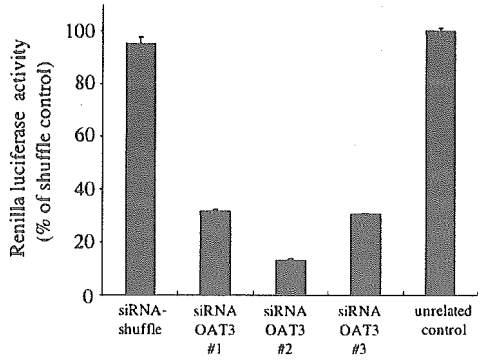

Fig. 1. Effect of siRNAs directed against the OAT3 in vitro. HEK293 cells were transfected with *Renilla* luciferase-fused OAT3 expression vector, *firefly* luciferase expression vector, and 25 nM siRNA. Reduction effect of *Renilla* luciferase activity relative to *firefly* luciferase activity was analyzed. Negative controls were the siRNA with randomized sequence of siRNA OAT3 #2 (siRNA-shuffle) and the siRNA against unrelated gene. Data were averaged from three experiments with SEM indicated.

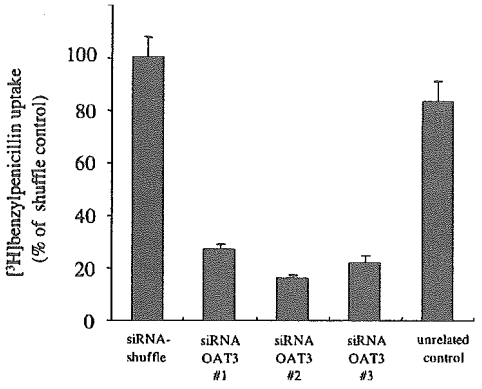

Fig. 2. Effect of siRNAs on uptake of OAT3 substrate in culture cells. Effect of siRNAs OAT3 on the OAT-3-mediated [^{3}H]benzylpenicillin uptake in HEK293 cells. After expression of OAT3 to the cells, [^{3}H]benzylpenicillin uptake was performed at 2 min, reflecting the initial uptake phase. All siRNAs were used at a concentration of 100 nM. Each value represents the mean ± SEM ($n = 4$). The increased uptake by expression of OAT3 was significantly reduced by siRNA OAT3 compared to siRNA-shuffle and siRNA-unrelated control. ($p < 0.0001$).

to HEK293 cells, the uptake mediated OAT3 was increased, and siRNA OAT3 #2 significantly inhibited the increased uptake of the substrate in HEK293 cells, compared with siRNA-shuffle and siRNA-unrelated control (Fig. 2).

In vivo delivery of siRNA to brain endothelial cells

We biochemically investigated an inhibitory effect of siRNA on expression of endogenous protein in BCECs using brain vascular fraction of small vessels from mouse brain.

For detection of endogenous protein in BCECs, we used SOD1 and siRNA to SOD1, because we have confirmed the efficient in vivo effect of this siRNA to endogenous mouse SOD1 in the siRNA-overexpressed transgenic mouse [14].

Western blot of the mouse brain small vascular fraction showed a reduction of endogenous mouse SOD1 level after hydrodynamic injection of siRNA SOD1 (Fig. 3A, left), whereas SOD1 level in the total homogenate of brain did not change (data not shown). There was a potentially more significant level of reduction on a per-BCEC basis, because the brain small vascular fraction contained proteins from cells other than BCECs such as pericytes and astrocytes [15]. We roughly estimated the content of BCECs in the brain small vascular fraction by performing a Western blot analysis with antibody to glucose-transporter-1 (GLUT-1) which specifically expressed in BCECs (Fig. 3B). The band intensity of GLUT-1 in the brain small vascular fraction was 4.1 (± 0.58) times more than that in mouse brain capillary endothelial cell lines which we previously established [12] (Fig. 3B). Since the cell line contains more than 1/8 of GLUT-1 [12], around 50% protein of the brain small vascular fraction that we made was supposed to come from brain endothelial cells.

In contrast, there was not obvious reduction of SOD1 level in the small vascular fraction after a regular intrave-

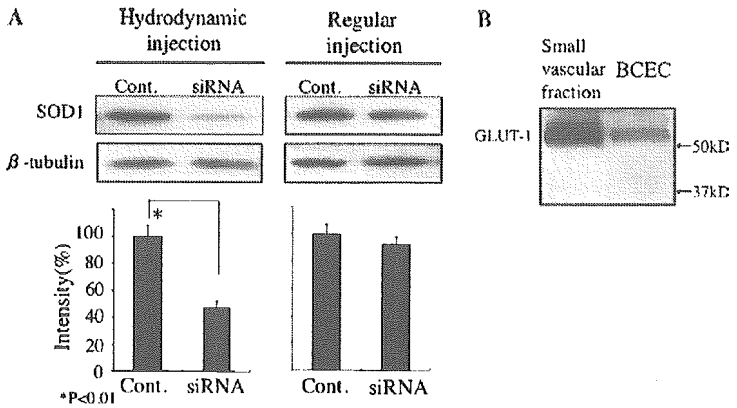

Fig. 3. Western blot analysis of mouse brain capillary-rich fraction. (A) The mouse brain small vascular fraction was examined on Western blot analysis after hydrodynamic (left) and regular (right) injection of 50 μg siRNA SOD1. The lower panels indicate percentages of signal intensities of SOD1 normalized with that of tubulin. (B) Western blot analysis with 2.5 μg protein of anti-GLUT-1 antibody of the mouse brain small vascular fraction (left) and mouse brain capillary endothelial cell lines (right). Signal intensity of GLUT-1 in the mouse brain small vascular fraction is 4.1 (± 0.58) times more than that in mouse brain capillary endothelial cell lines. BCEC, brain capillary endothelial cell line cells.

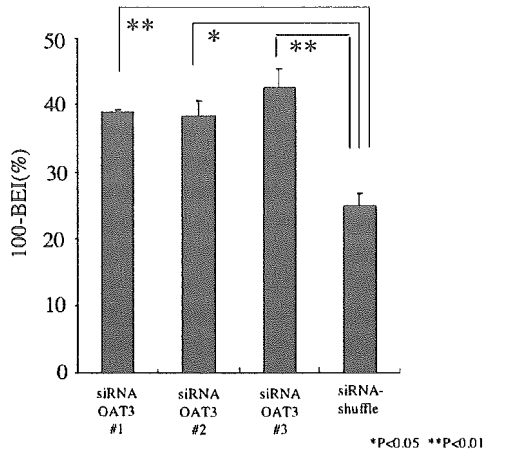

Fig. 4. Effect of siRNA on transport function of OAT3 by BEI. The 50 μg siRNA dissolved in the 5–10% volume PBS of mouse body weight was rapidly injected into the tail vein 36 h before the BEI assay. The residual radioactivity of OAT3 substrate, [^{3}H]benzylpenicillin in the brain, was measured at 40 min after intracerebral injection.

nous injection (Fig. 3A, right). These results indicate that hydrodynamic injection method is effective for delivery of siRNA to brain capillary endothelial cells.

In vivo effect of siRNA on transporter function of OAT3 in vivo

The in vivo inhibitory effect of siRNA OAT3 on the brain-to-blood efflux transport was examined with BEI method with intracerebral injection of OAT3 substrate, [^{3}H]benzylpenicillin. We intravenously injected siRNA OAT3 #2 to 11 mice, siRNA OAT3 #1 and #3 to 3 mice each, and siRNA-shuffle (control) to 7 mice with hydrodynamic method. Transport function of OAT3 was evaluated by BEI method at 36 h after the injection of siRNA. The results of 100-BEI, percentage of OAT3 substrate remaining in the brain after injection, are shown in Fig. 4. The value of 100-BEI of siRNA OAT3 #2 is significantly higher than that of siRNA-shuffle by 26.4%. Those of siRNA OAT3 #1 and #3 were also similarly higher than that of control. The results that plural different siRNAs to the OAT3 gene similarly increased 100-BEI value indicated that these siRNA influences were not "off-target effect" on molecules other than OAT3 in the brain. Taken together, these results suggested that in vivo applied-siRNA to OAT3 could suppress the brain-to-blood efflux function of OAT3.

Discussion

This is the first report of successful in vivo inhibition of endogenous gene in BCECs by systemic intravenous injection of siRNA. Furthermore, we demonstrated that our gene silencing effect was enough to suppress the transport function of OAT3 endogenously expressed in BCECs at BBB. We could deliver siRNA to BCECs by hydrodynamic injection method, but not by regular intravenous injection from the mouse tail vein. It has been thought that a rapid injection of a large bolus of solution develops a high pressure in the inferior vena cava, causing retrograde movement of the solution to the abdominal organs including liver and kidneys. Such a sharp increase in venous pressure enlarges the liver fenestrae and promotes membrane permeability of the hepatocytes, making siRNA enter the cells [16]. Since BCECs are circulated from the tail vein via lung capillary, the phasic hydrodynamic pressure in the inferior vena cava should decrease in the lung. However, rapid loading of extremely large volume of solution, 40–80% of circulating plasma volume should considerably increase hydrostatic pressure in the carotid artery due to volume overload. In addition, the rapid injection of large volume solution prevents the solution from being mixed with the serum containing RNase and keeps the concentration of siRNA extremely high when it is delivered to BCECs.

This in vivo knockdown method with siRNA to BCECs is expected to be a powerful tool for investigating function of BBB. The BBB is formed by the tight intercellular junctions of BCECs and regulates CNS homeostasis and drug delivery by restricting the transfer of substances between the circulating blood and the brain [17]. We have developed Brain Efflux Index as a reliable in vivo method of analyzing efflux transport at the BBB [18]. The efflux function of a transporter protein expressed in BCECs, such as OAT3, can be well evaluated by combining in vivo knockdown method with siRNA and BEI method.

Since synthetic siRNA does not work in the cells for no more than six days [19], long-term silencing of the target gene is necessary for investigating other functions of BCECs in the pathophysiology of atherosclerosis and Alzheimer's disease. Long-standing gene suppression can be achieved in vivo with adenovirus and adeno-associated virus (AAV) vectors expressing short hairpin RNA (shRNA) [20,21]. Actually, with the adenovirus expressing shRNA to SOD1 gene (2.0×10^9 pfu), we could efficiently suppress the endogenous SOD1 level of brain capillary-rich fraction by regular intravenous injection into mouse tail vein (unpublished data). For the evaluation of BCEC function, however, the AAV may be better than adenovirus, because BBB function should be less affected due to limited local immune response to the AAV capsid [22].

The hydrodynamic injection does not cause marked injury to organs in the animals [23], but it is hard to be clinically applied to patients because of its extremely high hydrostatic pressure and volume overload. Possible alternate is a regional delivery of large dose siRNA into carotid artery, but development of less invasive systemic delivery system in vivo is necessary for a therapeutic application of siRNA. Novel cationic liposomes have been reported to transduce efficiently siRNA into the liver [24] as well as tumor tissue [25]. These siRNAs formulated with cationic liposomes also induce interferons and cytokines in vivo through toll-like receptors [26,27] which should change the BBB function. Recently, the lipid-conjugated siRNA

at the 5′-end of the sense strand enhanced cellular uptake and gene silencing [28]. Combined with chemical modification of 2′-O-methylation and phosphorothioate to stabilize siRNA, substantial gene silencing in the liver and jejunum was achieved by a regular intravenous injection into the mouse tail vein [29]. Now, we are trying to use these new siRNA delivery methods to achieve more effective, stable, and safe gene suppression in BCECs for a clinical application.

Acknowledgments

We thank Dr. Tadashi Kanouchi and Miss Tsubura Takahashi for their help. This work was supported by grants from the Ministry of Education, Science and Culture of Japan and from the Ministry of Health, Labor and Welfare of Japan.

References

[1] R. Paul, Z.G. Zhang, B.P. Eliceiri, Q. Jiang, A.D. Boccia, R.L. Zhang, M. Chopp, D.A. Cheresh, Src deficiency or blockade of Src activity in mice provides cerebral protection following stroke, Nat. Med. 7 (2001) 222–227.

[2] C.J. Frijns, L.J. Kappell, Inflammatory cell adhesion molecules in ischemic cerebrovascular disease, Stroke 33 (2002) 2115–2122.

[3] J.J. Archelos, S. Jung, M. Mäurer, M. Schmied, H. Lassmann, T. Tamatani, M. Miyasaka, K.V. Toyka, H.P. Hartung, Inhibition of experimental autoimmune encephalomyelitis by an antibody to the intercellular adhesion molecule ICAM-1, Ann. Neurol. 34 (1993) 145–154.

[4] G.J. del Zoppo, T. Mabuchi, Cerebral microvessel responses to focal ischemia, J. Cereb. Blood Flow Metab. 23 (2003) 879–894.

[5] D.H. Miller, O.A. Khan, W.A. Sheremata, L.D. Blumhardt, G.P. Rice, M.A. Libonati, A.J. Willmer-Hulme, C.M. Dalton, K.A. Miszkiel, P.W. O'Connor, International Natalizumab Multiple Sclerosis Trial Group, A controlled trial of natalizumab for relapsing multiple sclerosis, N. Engl. J. Med. 348 (2003) 15–23.

[6] P.H. Chan, Reactive oxygen radicals in signaling and damage in the ischemic brain, J. Cereb. Blood Flow Metab. 21 (2001) 2–14.

[7] S. Hori, S. Ohtsuki, M. Ichinowatari, T. Yokota, T. Kanda, T. Terasaki, Selective gene silencing of rat ATP-binding cassette G2 transporter in an in vitro blood-brain barrier model by short interfering RNA, J. Neurochem. 93 (2005) 63–71.

[8] S. Ohtsuki, T. Kikkawa, S. Mori, S. Hori, H. Takanaga, M. Otagiri, T. Terasaki, Mouse reduced in osteosclerosis transporter function as an organic anion transporter 3 and is localized at albuminal membrane of blood-brain barrier, J. Pharmacol. Exp. Ther. 309 (2004) 1273–1281.

[9] F. Liu, Y.K. Song, D. Liu, Hydrodynamics-based transfection in animals by systemic administration of plasmid DNA, Gene Ther. 6 (1999) 1258–1266.

[10] T. Yokota, K. Igarashi, T. Uchihara, K. Jishage, H. Tomita, A. Inaba, Y. Li, M. Arita, H. Suzuki, H. Mizusawa, H. Arai, Delayed-onset ataxia in mice lacking alpha-tocopherol transfer protein: model for neuronal degeneration caused by chronic oxidative stress, Proc. Natl. Acad. Sci. USA 98 (2001) 15185–15190.

[11] T. Kanda, H. Yoshino, T. Ariga, M. Yamawaki, R.K. Yu, Glycosphingolipid antigens in cultured microvascular bovine brain endothelial cells: sulfoglucuronyl paragloboside as a target of monoclonal IgM in demyelinative neuropathy, J. Cell Biol. 126 (1994) 235–246.

[12] K. Hosoya, K. Tetsuka, K. Nagase, M. Tomi, S. Saeki, S. Ohtsuki, T. Terasaki, Conditionally immortalized brain capillary endothelial cell lines established from a transgenic mouse harboring temperature-sensitive Simian Virus 40 large T-antigen gene, AAPS Pharmsci. 2 (2000), [article 27].

[13] A. Kakee, T. Terasaki, Y. Sugiyama, Brain efflux index as a novel method of analyzing efflux transport at the blood-brain barrier, J. Pharmacol. Exp. Ther. 277 (1996) 1550–1559.

[14] Y. Saito, T. Yokota, T. Mitani, K. Ito, M. Anzai, M. Miyagishi, K. Taira, H. Mizusawa, Trangenic small interfering RNA halts amyotrophic lateral sclerosis in a mouse model, J. Biol. Chem. 2005 (in press).

[15] T. Kanda, T. Ariga, H. Kubodera, H.L. Jin, K. Owada, T. Kasama, M. Yamawaki, H. Mizusawa, Glycosphingolipid composition of primary cultured human brain microvascular endothelial cells, J. Neurosci. Res. 78 (2004) 141–150.

[16] G. Zhang, X. Gao, Y.K. Song, R. Vollmer, D.B. Stolz, J.Z. Gasiorowski, D.A. Dean, D. Liu, Hydroporation as the mechanism of hydrodynamic delivery, Gene Ther. 11 (2004) 675–682.

[17] K. Hosoya, S. Ohtsuki, T. Terasaki, Recent advances in the brain-to-blood efflux transport across the blood-brain barrier, Int. J. Pharm. 248 (2002) 15–29.

[18] T. Terasaki, S. Ohtsuki, S. Hori, H. Takanaga, E. Nakashima, K. Hosoya, New approaches to in vitro models of blood-brain barrier drug transport, Drug Discov. Today 8 (2003) 944–954.

[19] S.M. Elbashir, J. Harborth, W. Lendeckel, A. Yalcin, K. Weber, T. Tuschl, Duplexes of 21-nucleotide RNAs mediate RNA interference in cultured mammalian cells, Nature 411 (2001) 494–498.

[20] H. Xia, Q. Mao, H.L. Paulson, B.L. Davidson, siRNA-mediated gene silencing in vitro and in vivo, Nat. Biotechnol. 20 (2002) 1006–1010.

[21] H. Xia, Q. Mao, S.L. Eliason, S.Q. Harper, I.H. Martins, H.T. Orr, H.L. Paulson, L. Yang, R.M. Kotin, B.L. Davidson, RNAi suppresses polyglutamine-induced neurodegeneration in a model of spinocerebellar ataxia, Nat. Med. 10 (2004) 816–820.

[22] M.G. Kaplitt, P. Leone, R.J. Samulski, X. Xiao, D.W. Pfaff, K.L. O'Malley, M.J. During, Long-term gene expression and phenotypic correction using adeno-associated virus vectors in the mammalian brain, Nat. Genet. 8 (1994) 148–154.

[23] J.E. Knapp, D. Liu, Hydrodynamic delivery of DNA, Methods Mol. Biol. 245 (2004) 245–250.

[24] D.R. Sorensen, M. Leirdal, M. Sioud, Gene silencing by systemic delivery of synthetic siRNAs in adult mice, J. Mol. Biol. 327 (2003) 761–766.

[25] J. Yano, K. Hirabayashi, S. Nakagawa, T. Yamaguchi, M. Nogawa, I. Kashimori, H. Naito, H. Kitagawa, K. Ishiyama, T. Ohgi, T. Irimura, Antitumor activity of small interfering RNA/cationic liposome complex in mouse models of cancer, Clin. Cancer Res. 10 (2004) 7721–7726.

[26] A.D. Judge, V. Sood, J.R. Shaw, D. Fang, K. McClintock, I. MacLachlan, Sequence-dependent stimulation of the mammalian innate immune response by synthetic siRNA, Nat. Biotechnol. 23 (2005) 457–462.

[27] V. Hornung, M. Guenthner-Biller, C. Bourquin, A. Ablasser, M. Schlee, S. Uematsu, A. Noronha, M. Manoharan, S. Akira, A. de Fougerolles, S. Endres, G. Hartmann, Sequence-specific potent induction of IFN-alpha by short interfering RNA in plasmacytoid dendritic cells through TLR7, Nat. Med. 11 (2005) 263–270.

[28] C. Lorenz, P. Hadwiger, M. John, H.P. Vornlocher, C. Unverzagt, Steroid and lipid conjugates of siRNAs to enhance cellular uptake and gene silencing in liver cells, Bioorg. Med. Chem. Lett. 14 (2004) 4975–4977.

[29] J. Soutschek, A. Akinc, B. Bramlage, K. Charisse, R. Constien, M. Donoghue, S. Elbashir, A. Geick, P. Hadwiger, J. Harborth, M. John, V. Kesavan, G. Lavine, R.K. Pandey, T. Racie, K.G. Rajeev, I. Rohl, I. Toudjarska, G. Wang, S. Wuschko, D. Bumcrot, V. Koteliansky, S. Limmer, M. Manoharan, H.P. Vornlocher, Therapeutic silencing of an endogenous gene by systemic administration of modified siRNAs, Nature 432 (2004) 173–178.

ELSEVIER

Journal of Neuroscience Methods xxx (2005) xxx–xxx

JOURNAL OF NEUROSCIENCE METHODS

www.elsevier.com/locate/jneumeth

Rapid identification of 14-3-3-binding proteins by protein microarray analysis

Jun-ichi Satoh[a,b,*], Yusuke Nanri[a], Takashi Yamamura[a]

[a] *Department of Immunology, National Institute of Neuroscience, NCNP, 4-1-1 Ogawahigashi, Kodaira, Tokyo 187-8502, Japan*

[b] *Department of Bioinformatics and Neuroinformatics, Meiji Pharmaceutical University, 2-522-1 Noshio, Kiyose, Tokyo 204-8588, Japan*

Received 8 June 2005; received in revised form 19 September 2005; accepted 26 September 2005

Abstract

The 14-3-3 protein family consists of acidic 30-kDa proteins composed of seven isoforms in mammalian cells, expressed abundantly in neurons and glial cells of the central nervous system (CNS). The 14-3-3 isoforms form a dimer that acts as a molecular adaptor interacting with key signaling components involved in cell proliferation, transformation, and apoptosis. Until present, more than 300 proteins have been identified as 14-3-3-binding partners, although most of previous studies focused on a limited range of 14-3-3-interacting proteins. Here, we studied a comprehensive profile of 14-3-3-binding proteins by analyzing a high-density protein microarray using recombinant human 14-3-3 epsilon protein as a probe. Among 1752 proteins immobilized on the microarray, 20 were identified as 14-3-3 interactors, most of which were previously unreported 14-3-3-binding partners. However, 11 known 14-3-3-binding proteins, including keratin 18 (KRT18) and mitogen-activated protein kinase-activated protein kinase 2 (MAPKAPK2), were not identified as a 14-3-3-binding protein. The specific binding to 14-3-3 of EAP30 subunit of ELL complex (EAP30), dead box polypeptide 54 (DDX54), and src homology three (SH3) and cysteine rich domain (STAC) was verified by immunoprecipitation analysis of the recombinant proteins expressed in HEK293 cells. These results suggest that protein microarray is a powerful tool for rapid and comprehensive profiling of 14-3-3-binding proteins.

Keywords: 14-3-3-Binding protein; Immunoprecipitation; Protein microarray; Protein–protein interaction; STAC

1. Introduction

The 14-3-3 protein family consists of evolutionarily conserved, acidic 30-kDa proteins composed of seven isoforms named β, γ, ε, ζ, η, θ, and σ in mammalian cells. A homodimeric or heterodimeric complex composed of the same or distinct isoforms constitutes a large cup-like structure possessing an amphipathic groove with two ligand-binding capacity (Fu et al., 2000; van Hemert et al., 2001). The dimeric complex acts as a molecular adaptor that interacts with key signaling molecules involved in cell differentiation, proliferation, transformation, and apoptosis. It regulates the function of target proteins by restricting their subcellular location, bridging them to modulate catalytic activity, and protecting them from dephosphorylation or proteolysis (Dougherty and Morrison, 2004; MacKintosh, 2004). Although 14-3-3 is widely distributed in neural and non-neural tissues, it is expressed most abundantly in neurons in the central nervous system (CNS), where it represents 1% of total cytosolic proteins (Berg et al., 2002). Aberrant expression and impaired function of 14-3-3 in the CNS are associated with pathogenetic mechanisms of Creutzfeldt–Jacob disease, Alzheimer disease, Parkinson disease, spinocerebellar ataxia, amyotrophic lateral sclerosis, and multiple sclerosis (Chen et al., 2003; Kawamoto et al., 2002; Layfield et al., 1996; Malaspina et al., 2000; Satoh et al., 2004; Zerr et al., 1998).

In general, the 14-3-3 protein interacts with phosphoserine-containing motifs of the ligands such as RSXpSXP (mode I) and RXXXpSXP (mode II) in a sequence-specific manner (Dougherty and Morrison, 2004; MacKintosh, 2004). Previously, more than 300 proteins have been identified as being 14-3-3-binding partners. They include key signaling components, such as Raf-1 kinase, Bcl-2 antagonist of cell death (BAD), protein kinase C (PKC), phophatidylinositol 3-kinase (PI3K), and cdc25 phosphatase (Fu et al., 2000; van Hemert et al., 2001). Binding of 14-3-3 to Raf-1 is indispensable for its kinase activity in the Ras-MAPK signaling pathway, and the interaction of 14-3-3 with BAD, when phosphorylated by

* Corresponding author. Tel.: +81 42 341 2711; fax: +81 42 346 1753.
E-mail address: satoj@ncnp.go.jp (J.-i. Satoh).

0165-0270/$ – see front matter © 2005 Published by Elsevier B.V.
doi:10.1016/j.jneumeth.2005.09.015

a serine/threonine kinase Akt, inhibits apoptosis. Recent studies indicate that the 14-3-3 protein could interact with a set of target proteins in a phosphorylation-independent manner (Dai and Murakami, 2003; Henriksson et al., 2002; Zhai et al., 2001). Increasing knowledge of interactions between 14-3-3 and interacting molecules would help us to understand the biological function and pathological implication of the 14-3-3 protein networks.

The yeast two-hybrid (Y2H) system is a powerful approach to identify novel protein–protein interactions. However, Y2H screening requires a lot of time and effort, and is often criticized for detecting the interactions unrelated to the physiological setting and obtaining high rates of false positive interactors caused by spontaneous activation of reporter genes and self-activating bait proteins (Vidalain et al., 2004; Zhang et al., 2004). Affinity purification coupled with mass spectrometry (APMS) is an alternative approach to identify the components of protein complexes on a large scale. This approach has been taken to identify a wide variety of 14-3-3-interacting proteins involved in cell proliferation, metabolism, and survival (Benzinger et al., 2005; Jin et al., 2004; Meek et al., 2004; Pozuelo Rubio et al., 2004). Although the APMS procedure detects binding partners of physiological significance, it is laborious and has a difficulty in detecting transmembrane proteins and loosely associated components that might be lost during purification (von Mering et al., 2002). Recently, protein microarray technology has been established for rapid, systematic, and less expensive screening of thousands of protein–protein, protein–lipid, and protein–nucleic acid interactions in a high-throughput fashion. This approach has important applications in the areas not only of basic biological research but also of drug discovery research, including identification of the substrates of protein kinases and the protein targets of small molecules (Chan et al., 2004; MacBeath and Schreiber, 2000; Michaud et al., 2003; Zhu et al., 2001).

The present study was designed for the first time to identify a comprehensive profile of human 14-3-3-binding proteins by analyzing a high-density protein microarray.

2. Materials and methods

2.1. Preparation of a probe for microarray analysis

Human embryonic kidney cells HEK293 whose genome was modified for the Flp-In system (Flp-In 293) were obtained from Invitrogen, Carlsbad, CA. Flp-In 293 cells contain a single Flp recombination target (FRT) site targeted for the site-specific recombination, integrated in a transcriptionally active locus of the genome, where it stably expresses the *lac*Z-Zeocin fusion gene driven from the pFRT/*lac*Zeo plasmid under the control of SV40 early promoter. Flp-In 293 cells were maintained in Dulbecco's modified Eagle's medium (DMEM) supplemented with 10% fetal bovine serum (FBS), 100 U/ml of penicillin, and 100 μg/ml of streptomycin (feeding medium) with inclusion of 100 μg/ml of Zeocin (Invitrogen) as described previously (Satoh and Yamamura, 2004).

To prepare the probe for protein microarray analysis, the open reading frame (ORF) of the human 14-3-3ε gene (YWHAE) was amplified from cDNA of NTera2-N cells (Satoh and Kuroda, 2000) by PCR using PfuTurbo DNA polymerase (Stratagene, La Jolla, CA, USA) and the primer sets listed in Table 1. The PCR product was then cloned into a mammalian expression vector pSecTag/FRT/V5-His TOPO (Invitrogen) to produce a fusion protein with a C-terminal V5 (GKPIPNPLLGLDST) tag, a C-terminal polyhistidine (6 × His) tag, and an N-terminal Ig κ-chain secretion signal. This vector, together with the Flp recombinase expression vector pOG44 (Invitrogen), was transfected in Flp-In 293 cells by Lipofectamine 2000 reagent (Invitrogen). A stable cell line was established after incubating the transfected cells for approximately 1 month in the feeding medium with inclusion of 100 μg/ml of Hygromycin B (Invitrogen). It was named 293 eV5. The recombinant protein was secreted into the culture medium of 293 eV5 cells after the Ig κ-chain secretion signal sequence was processed by an endogenous signal peptidase-mediated cleavage.

To purify the recombinant 14-3-3ε protein, the culture supernatant of 293 eV5 cells incubated for 48 h in the serum-free DMEM/F-12 medium was harvested and concentrated at an 1/40 volume by centrifugation on an Amicon Ultra-15 filter (Millipore, Bedford, MA). It was then purified by the HIS-select spin column (Sigma, St. Louis, MO) and concentrated at an 1/10 volume by centrifugation on a Centricon-10 filter (Millipore). The protein concentration was determined by a Bradford assay kit (BioRad, Hercules, CA). The purity and specificity of the probe were verified by Western blot analysis using mouse monoclonal anti-V5 antibody (Invitrogen) and rabbit polyclonal antibody specific for the 14-3-3ε isoform (IBL, Gumma, Japan).

2.2. Protein microarray analysis

ProtoArray human protein microarray (v1.0) commercially available from Invitrogen was utilized in the present study. It contains 1752 human proteins of various functional classes spotted in duplicate on a nitrocellulose-coated glass slide. To prepare target proteins immobilized on the microarray, an N-terminal glutathione-*S* transferase (GST)-6× His fusion protein derived from the genes selected from the human ultimate ORF clone collection (Invitrogen) was expressed in Sf9 insect cells by using the baculovirus expression system (Invitrogen). Either the full-length or the partial fragment of recombinant proteins, was purified under native conditions by glutathione affinity chromatography in the presence of protease inhibitors, then processed for spotting on the slides. The proteins were printed in an arrangement composed of 4 × 12 subarrays equally spaced in vertical and horizontal directions (Fig. 1a). Each subarray included 16 × 16 spots, composed of 48 control spots (C), 80 human proteins (H), and 128 blanks (B) (Fig. 1c). The control proteins (C) were composed of 14 positive control spots and 34 negative control spots. The former includes four spots of an Alexa Fluor 647-labeled antibody (rows 1, 8; columns 1, 2), six spots of a concentration gradient of a biotinlyated anti-mouse antibody with a capacity to bind to mouse monoclonal anti-V5 antibody conjugated with Alexa Fluor 647 (row 8; columns 3–8), and four spots of a concentration gradient of V5 protein (row 8; columns 13–16). The latter includes six spots of a concentra-

Table 1
Primers utilized for PCR-based cloning and site-directed mutagenesis

Genes	Proteins (amino acid residues)	GenBank accession no.	Sense primers	Antisense primers	Cloning vector
YWHAE	14-3-3ε Isoform (2-255)	NM_006761	5′gatgatcgaggatctggtgtac3′	5′ctgatttttgtctttccacgttctg3′	pSecTag/FRT/V5-His TOPO
EAP30	EAP30 subunit of ELL complex (2-258)	NM_007241	5′caccgcgcgggtggaagctggc3′	5′tcagggaggggcttctctggcctc3′	pcDNA4/HisMax-TOPO
DDX54	Dead box polypeptide 54 (2-881)	NM_024072	5′gcggccgcacaaggcccggcggct3′	5′tcacatcctcttccgcatcttgcc3′	pcDNA4/HisMax-TOPO
STAC	src homology three and cysteine rich domain (2-402, full length)	NM_003149	5′atccctccgagcagcccccgcgag3′	5′tcagatgttttctagtacatcaag3′	pcDNA4/HisMax-TOPO
STAC	src homology three and cysteine rich domain (2-402 with S172A: SMT)	NM_003149	5′gtttcggcgttactacgcctcccctt-gctcattc3′	5′gaatgagcaagggggaggcgtagtaa-cgccgaaac3′	pcDNA4/HisMax-TOPO modified by site-directed mutagenesis
STAC	src homology three and cysteine rich domain (2-402 with S172A and S173A: DMT)	NM_003149	5′cggcgttactacgccgccccctt-gctcattcat3′	5′atgaatgagcaagggggcggcgt-agtaacgccg3′	pcDNA4/HisMax-TOPO modified by site-directed mutagenesis
STAC	src homology three and cysteine rich domain (2-233. N-terminal half: NTF)	NM_003149	5′atccctccgagcagcccccgcgag3′	5′tcaaagatctgaagtagaggttct3′	pcDNA4/HisMax-TOPO
STAC	src homology three and cysteine rich domain (234-402. C-terminal half: CTF)	NM_003149	5′gtggaggttcctgaggaagccaat3′	5′tcagccacctggatgcagaccagc3′	pcDNA4/HisMax-TOPO
STAC	src homology three and cysteine rich domain (2-164. truncated form A: TR-A)	NM_003149	5′atccctccgagcagcccccgcgag3′	5′tcatggcagcttgcccatgcaccg3′	pcDNA4/HisMax-TOPO
STAC	src homology three and cysteine rich domain (2-105. truncated form B; TR-B)	NM_003149	5′atccctccgagcagcccccgcgag3′	5′tcagccacctggatgcagaccagc3′	pcDNA4/HisMax-TOPO

The PCR product was cloned into a vector pSecTag/FRT/V5-His TOPO to express a fusion protein with a V5 tag or into a vector pcDNA4/HisMax-TOPO to express a fusion protein with a Xpress tag in HEK293 cells.

tion gradient of bovine serum albumin (BSA) (row 1; columns 3–8), four spots of a concentration gradient of a rabbit anti-GST antibody (row 1; columns 9–12), four spots of a concentration gradient of calmodulin (row 1; columns 13–16), 16 spots of a concentration gradient of GST (row 2; columns 1–16), two spots of buffer only (row 8; columns 9,10), and two spots of an anti-biotin antibody (row 8; columns 11,12). The complete list of 1752 target proteins immobilized on the microarary is shown in Supplementary Table 1 online.

Non-specific binding was blocked by incubating the microarray for 90 min in the PBST blocking buffer composed of 1% BSA and 0.1% Tween 20 in phosphate-buffered saline (PBS). Then, it was incubated for 30 min at 4 °C with the probe described above at a concentration of 50 μg/ml in the probing buffer composed of 1% BSA, 5 mM $MgCl_2$, 0.5 mM dithiothreitol (DTT), 0.05% Triton X-100, and 5% glycerol in PBS. The array was washed three times with the probing buffer, followed by incubation for 30 min at 4 °C with mouse monoclonal anti-V5 antibody conjugated with Alexa Fluor 647 (Invitrogen) at a concentration of 260 ng/ml in the probing buffer. The array was washed three times with the probing buffer, and then scanned by the GenePix 4200A scanner (Axon Instruments, Union City, CA) at a wavelength of 635 nm. The data were analyzed by using the ProtoArray Prospector software v2.0 (Invitrogen) following acquisition of the microarray lot-specific information online, including inter-lot variations in protein concentrations (http://www.invitrogen.com/protoarray). According to the default setting of the software, the spots showing the background-subtracted signal intensity value greater than the median plus three standard deviations of all the fluorescence intensities were considered as having a significant binding. The Z-score, an indicator for statistical evaluation of binding specificity, was calculated as the background-subtracted signal intensity value of the target protein minus the average of the background-subtracted signal intensity value from the negative control distribution, divided by the standard deviation of the negative control distribution. All the procedure described above could be accomplished within 5 h. The 14-3-3-binding consensus motif mode I (RSXpSXP) sequence located in target proteins was surveyed by the Scansite Motif Scanner, which assesses the probability of a site matching the candidate motif under high, medium, or low stringent conditions (Obenauer et al., 2003). The information on known 14-3-3 interactors was obtained from Biomolecular Interaction Network Database (BIND; http://www.bind.ca) and PubMed database search.

2.3. Transient expression of 14-3-3-binding proteins in HEK293 cells

To verify the results of microarray analysis, the ORF of the genes encoding EAP30 subunit of ELL complex (EAP30), dead box polypeptide 54 (DDX54), and src homology three (SH3) and cysteine rich domain (STAC) were amplified by PCR using PfuTurbo DNA polymerase and the primer sets listed in Table 1. They were then cloned into a mammalian expression vector pcDNA4/HisMax-TOPO (Invitrogen) to produce a fusion protein with an N-terminal Xpress tag. To express the STAC mutant

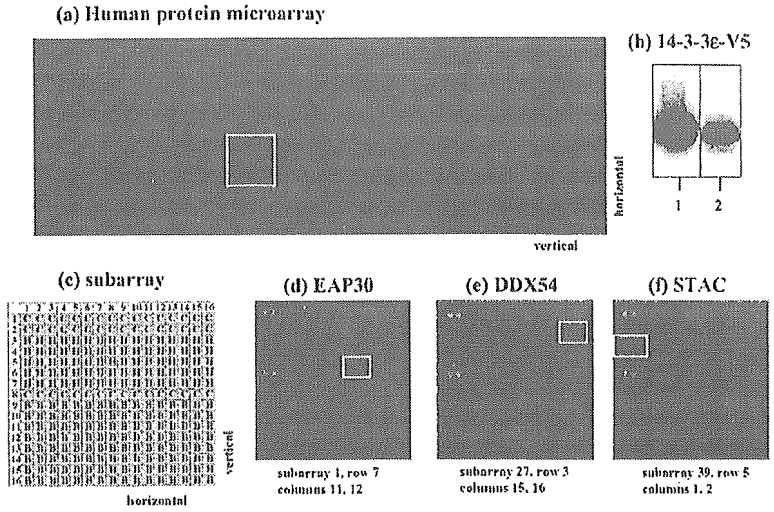

Fig. 1. Protein microarray analysis. (a) Human protein microarray. The microarray contains 1752 distinct human proteins of various functional classes spotted in duplicate on a nitrocellulose-coated glass slide. They are printed in an arrangement of 4 × 12 subarrays equally spaced in vertical and horizontal directions. A representative subarray is indicated by an enclosed yellow line. (b) Recombinant human 14-3-3ε protein tagged with V5. One microgram of the protein was processed for Western blot analysis using anti-V5 antibody (lane 1) or anti-14-3-3ε antibody (lane 2). (c) Layout of the subarray. Each subarray includes 16 × 16 spots composed of 48 control spots (C), 80 human proteins (H), and 128 blanks (B). The positive control spots include an Alexa Fluor 647-labeled antibody (rows 1, 8; columns 1, 2; strong signals), a concentration gradient of a biotinlyated anti-mouse antibody with a capacity to bind to mouse monoclonal anti-V5 antibody conjugated with Alexa Fluor 647 (row 8; columns 3–8; signals visible on the higher concentration), and a concentration gradient of V5 protein (row 8; columns 13–16; signals visible on the higher concentration). (d) EAP30. (e) DDX54. (f) STAC. The three proteins indicated by an enclosed yellow line located on different subarrays (d, f) represent an example identified as showing significant binding to the probe.

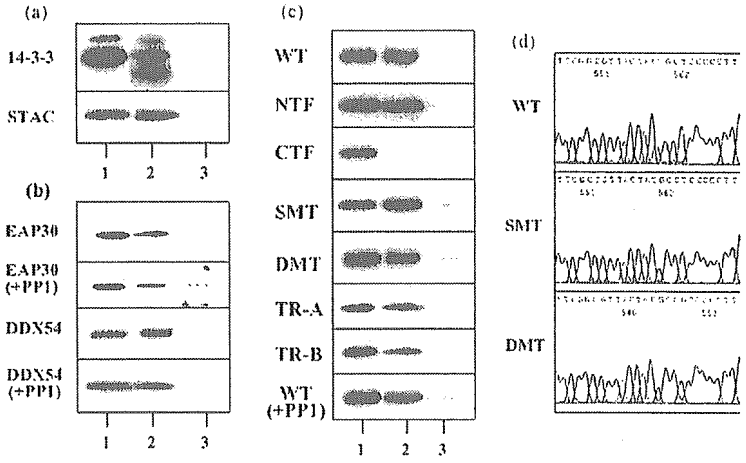

Fig. 2. Immunoprecipitation analysis of 14-3-3-binding proteins. (a) Binding of STAC to 14-3-3. Total protein extract of HEK293 cells expressing Xpress-tagged recombinant STAC was processed for immunoprecipitation (IP) with rabbit polyclonal antibody reacting with all 14-3-3 isoforms (K-19) or with normal rabbit IgG. The immunoprecipitates were then processed for Western blot analysis using mouse monoclonal antibody reacting with all 14-3-3 isoforms (H-8) (upper panel) or mouse monoclonal anti-Xpress antibody (lower panel). Lanes (1–3) represent (1) the input control, and IP with (2) K-19 and (3) normal rabbit IgG. (b) Binding of EAP30 and DDX54 to 14-3-3. Total protein of HEK293 cells expressing Xpress-tagged recombinant EAP30 or DDX54 extracted by using the lysis buffer with inclusion of phosphatase inhibitors or with inclusion of protein phosphatase-1 (PP1) instead of phosphatase inhibitors (+PP1) was processed for IP with K-19 or with normal rabbit IgG. The immunoprecipitates were then processed for Western blot analysis using anti-Xpress antibody. Lanes (1–3) represent (1) the input control, and IP with (2) K-19 and (3) normal rabbit IgG. (c) Binding of mutant and truncated STAC to 14-3-3. Total protein was extracted from HEK293 cells expressing a panel of Xpress-tagged recombinant STAC proteins. They include the full-length wild-type (WT) STAC, the N-terminal half (NTF), the C-terminal half (CTF), the S172A mutant (SMT), the S172A and S173A double mutant (DMT), the truncated form lacking the 14-3-3-binding consensus motif RYYSSP (TR-A), the truncated form lacking the cysteine-rich domain (CRD) (TR-B), and WT STAC isolated by using the lysis buffer with inclusion of PP1 instead of phosphatase inhibitors (WT + PP1). Primers utilized for PCR-based cloning and site-directed mutagenesis are listed in Table 1. The lysate was processed for IP with K-19 or with normal rabbit IgG. The immunoprecipitates were then processed for Western blot analysis using anti-Xpress antibody. Lanes (1–3) represent (1) the input control, and IP with (2) K-19 and (3) normal rabbit IgG. (d) The sequence of the 14-3-3-binding consensus motif located in amino acid residues 169-174 in expression vectors of STAC. The panels indicate WT (nucleotide sequence CGT-TAC-TAC-AGC-TCC-CCC: the corresponding amino acid sequence RYYSSP), SMT (CGT-TAC-TAC-GCC-TCC-CCC: RYYASP), and DMT (CGT-TAC-TAC-GCC-GCC-CCC: RYYAAP).

with a single amino acid substitution S172A (the single mutant; SMT) or with double amino acid substitutions S172A and S173A (the double mutant; DMT), the pcDNA4/HisMax-TOPO vector containing the wild-type (WT) STAC gene was modified by consecutive site-directed mutagenesis using QuikChange II site-directed mutagenesis kit (Stratagene) and the primer sets listed in Table 1. The mutations introduced in the vector were verified by sequencing analysis (Fig. 2d). All these vectors were transfected in HEK293 cells by Lipofectamine 2000 reagent.

2.4. Immunoprecipitation analysis

To prepare total protein extract, the cells were homogenized and incubated at room temperature for 30 min in M-PER lysis buffer (Pierce, Rockford, IL) supplemented with a cocktail of protease inhibitors (Sigma), with inclusion of phosphatase inhibitors (Sigma) to maintain the protein phosphorylation status or with inclusion of recombinant protein phosphatase-1 (PP1) catalytic subunit α-isoform (5 U/ml; Sigma) instead of phosphatase inhibitors to induce the protein dephosphorylation reaction (Ichimura et al., 2005), followed by centrifugation at 12,000 rpm at 4 °C for 20 min. After preclearance, the supernatant was incubated at 4 °C for 3 h with 30 μg/ml rabbit polyclonal anti-14-3-3 protein antibody (K19)-conjugated agarose (Santa Cruz Biotechnology, Santa Cruz, CA) or the same amount of normal rabbit IgG-conjugated agarose (Santa Cruz Biotechnology). After several washes, the immunoprecipitates were processed for Western blot analysis using mouse monoclonal anti-14-3-3 protein antibody (H-8, Santa Cruz Biotechnology) and mouse monoclonal anti-Xpress antibody (Invitrogen). K-19 and H-8 antibodies recognize all 14-3-3 isoforms. The specific reaction was visualized using a chemiluminescent substrate (Pierce).

3. Results

3.1. Protein microarray analysis identified 20 distinct 14-3-3-binding partners

To analyze a high-density human protein microarray, the recombinant 14-3-3ε protein tagged with V5 was purified form the supernatant of 293 eV5 cells secreting the recombinant protein in the culture medium. Western blot analysis verified the purity and specificity of the probe (Fig. 1b). Among 1752 proteins on the microarray, 20 were identified as the proteins showing significant binding to the probe (Table 2). All of these were previously unreported 14-3-3-binding partners by the BIND search. Seven were hypothetical clones of uncharacterized function, derived from the mammalian genome collection (MGC) or the full-length long Japan (FLJ). Thirteen annotated proteins included EAP30 subunit of ELL complex (EAP30) (Fig. 1d), lymphocyte cytosolic protein 2 (LCP2), methionine aminopeptidase 2 (METAP2), melanoma antigen family B, 4 (MAGEB4), chondroitin 4 sulfotransferase 11 (CHST11), nuclear interacting partner of anaplastic lymphoma kinase (ZC3HC1), minichromosome maintenance deficient 10 (MCM10), DEAD box polypeptide 54 (DDX54) (Fig. 1e), heterogeneous nuclear ribonucleoprotein C (HNPRC), fibroblast growth factor 12 (FGF12), glutathione *S*-transferase M3 (GSTM3), src homology three (SH3) and cysteine rich domain (STAC) (Fig. 1f), and ATPase, H+ transporting, lysosomal, 21 kDa, V0 subunit C″ (ATP6V0B). The 14-3-3-binding consensus motif mode I (RSX*p*SXP) was found only in STAC (*pS*172) and HNRPC (*pS*125) by the Scansite Motif Scanner search under the high stringent condition, while 15 of 20 proteins have one or several motifs when a query with the medium or low stringency was performed (Table 2).

3.2. Immunoprecipitation analysis validated the specific binding to 14-3-3

EAP30, DDX54, and STAC were selected to verify the results of microarray analysis, in view of their higher Z-scores. The recombinant proteins were expressed in HEK293 cells, which constitutively express a substantial amount of endogenous 14-3-3 protein. Total protein was extracted by using the lysis buffer with inclusion of phosphatase inhibitors to maintain the protein phosphorylation status or with inclusion of recombinant protein phosphatase-1 (PP1) instead of phosphatase inhibitors to induce the protein dephosphorylation reaction, followed by processing for immunoprecipitation (IP) with rabbit polyclonal antibody reacting with all 14-3-3 isoforms (K-19) or with normal rabbit IgG. K19 coimmunoprecipitated 14-3-3 and STAC from the lysate of HEK293 cells expressing the recombinant STAC protein, whereas normal rabbit IgG did not pull down these proteins (Fig. 2a). K-19 immunoprecipitated EAP30 and DDX54 from the lysate of HEK293 cells expressing the recombinant EAP30 or DDX54 protein, respectively, under both phosphorylated and dephosphorylated conditions (Fig. 2b). These results indicate that EAP30, DDX54, and STAC could interact with the endogenous 14-3-3 protein in HEK293 cells where the corresponding recombinant proteins were expressed.

STAC has the highly stringent 14-3-3-binding consensus motif RYYSSP in amino acid residues 169-174 (*pS*172), as suggested by the Scansite Motif Scanner (Table 2). Therefore, a possible involvement of this motif in binding to 14-3-3 was investigated by IP analysis of a series of mutant and truncated STAC proteins (Table 1). K-19 immunoprecipitated the full-length wild-type (WT) STAC comprised of amino acid residues 2-402 (Fig. 2a and c). K-19 also pulled down the S172A mutant (SMT), and the S172A and S173A double mutant (DMT), and the N-terminal half (NTF; amino acid residues 2-233) from the lysate of HEK293 cells expressing the corresponding recombinant proteins (Fig. 2c). In contrast, K-19 did not pull down the C-terminal half (CTF; amino acid residues 234-402) (Fig. 2c). These observations indicate that the RYYSSP motif is not essential for binding of STAC to 14-3-3. This was confirmed by the observations that K-19 immunoprecipitated the truncated form lacking the RYYSSP sequence (TR-A; amino acid residues 2-164) and the shortest form lacking both the RYYSSP sequence and the cysteine-rich domain (CRD) (TR-B; amino acid residues 2-105) from the lysate of HEK293 cells expressing the corresponding recombinant proteins (Fig. 2c). Finally, the full-length WT STAC interacted with 14-3-3 under the dephosphorylated condition (Fig. 2c). These observations indicate that the 14-